

current was significantly reduced in dnMEF2-transfected myocytes (Figure 6B, lower traces). Figure 6C outlines the current-voltage diagram. The amplitude of I_h in dnMEF2-transfected myocytes was ~18% of the control myocytes. Similar results were also obtained for ES-derived cardiomyocytes (data not shown).¹⁵

4. Discussion

The transcription factors AP1 and MEF2 are known to play a variety of roles in the development of the heart. It has been reported that the ablation of *c-jun*, who along with *c-fos* forms the AP1 transcription factor, gave rise to the anomalies of right ventricular outflow tract and a reduction in *Cx43* expression.¹⁶ Although we did not examine the direct physiological role of AP1 in the present study, it appears reasonable to expect that the expression of the *Hcn4* gene might also be reduced following the deletion of the AP1 protein. During development, *MEF2C* is known to be the predominant form of *MEF2* expressed in the embryonic heart. *MEF2A* and *MEF2D* became the major *MEF2* forms after birth.¹⁰ Gene knockout of *MEF2C* results in an embryonic lethal phenotype.¹⁷ *MEF2D*^{-/-} mice are viable, demonstrating a weak response to hypertrophic stimulation.¹⁸ *MEF2A* knockout mice generated on a 129Sv background die immediately following birth and demonstrate sinus arrhythmia and conduction block.¹⁹ As the present study demonstrates that the expression of *Hcn4* is dependent on *MEF2*, it would be interesting to explore the ion channel expression in SAN of *MEF2A*^{-/-} animals.

Recent studies have suggested that the *Nkx2-5* and *Pitx2c* transcription factors repress the expression of *Hcn4* in chamber myocardium, a result that is likely due to the inhibition of activators.¹⁶ However, activators of *Hcn4* have not been identified in cardiomyocytes to date. The results of the current study suggest that *MEF2* and *AP1* may be candidate activators. The transcription factor *Tbx3*, in addition to *Hcn4*, is also specifically expressed in SAN. Ectopic expression of *Tbx3* in the atrium is known to induce *Hcn4* expression. However, it remains unclear whether *Hcn4* is a direct target of *Tbx3*.⁵ Interestingly, we identified conserved *MEF2*- and *AP1*-like sequences within the *tbx3* gene locus. The spatiotemporal expression of *Tbx3* and *Hcn4* might be regulated via similar mechanisms.

MEF2 expression in the heart has been shown to be increased in the atrium.²⁰ Therefore, regional differences in *MEF2* expression might account in part for the spatial distribution of *Hcn4*. In this respect, it appears to be particularly important to investigate whether *CNS13* is able to reproduce the spatiotemporal expression pattern of *Hcn4* in the heart. Although we have generated transgenic mice harbouring a *LacZ* reporter gene driven by the *CNS13* and *Hcn4* promoter, we were unable to obtain consistent patterns of β -gal expression in embryos (data not shown). Thus, it is speculated that a combination of multiple *CNSs* may be required to reproduce the precise spatiotemporal expression pattern of *Hcn4*. Future studies will be required to address this question.

Supplementary material

Supplementary Material is available at *Cardiovascular Research* online.

Acknowledgements

We thank Dr M.A. Arnold for providing the dominant negative *MEF2* cDNA.

Conflict of interest: none declared.

Funding

This work was supported in part by a Grant from the Vehicle Racing Commemorative Foundation and a Grant-in-Aid for Scientific Research from JSPS (#20300141).

References

- Shram G, Pourrier M, Melnyk P, Nattel S. Differential distribution of cardiac ion channel expression as a basis for regional specialization in electrical function. *Circ Res* 2002;**90**:939-950.
- Marionneau C, Couette B, Liu J, Mangoni M-E, Nargoet J, Lei M *et al*. Specific pattern of ion channel gene expression associated with pacemaker activity in the mouse heart. *J Physiol* 2005;**562**:223-234.
- Ishii TM, Takano M, Xie L-H, Noma A, Ohmori H. Molecular characterization of the hyperpolarization-activated cation channel in rabbit heart sinoatrial node. *J Biol Chem* 1999;**274**:12835-12839.
- Hermann S, Stieber J, Ludwig A. Pathophysiology of HCN channels. *Pflugers Arch* 2007;**454**:517-522.
- Hoogaars W-M, Engel A, Brons J-F, Verkerk A-O, de Lange F-J, Wong L-Y *et al*. *Tbx3* controls the sinoatrial node gene program and imposes pacemaker function on the atria. *Genes Dev* 2007;**21**:1098-1112.
- Mommersteeg M-T, Hoogaars W-M, Prall O-W, de Gier-de Vries C, Wiese C, Clout D-E *et al*. Molecular pathway for the localized formation of the sinoatrial node. *Circ Res* 2007;**100**:354-362.
- Pennacchio L-A, Ahituv N, Moses A-M, Prabhakar S, Nobrega M-A, Shoukry M *et al*. In vivo enhancer analysis of human conserved non-coding sequences. *Nature* 2006;**444**:499-502.
- Visel A, Minovitsky S, Dubchak I, Pennacchio L-A. VISTA Enhancer Browser—a database of tissue-specific human enhancers. *Nucleic Acids Res* 2007;**35**:D88-D92.
- Kuratomi S, Kuratomi A, Kuwahara K, Ishii TM, Nakao K, Saito Y *et al*. *NRSF* regulates the developmental and hypertrophic changes of HCN4 transcription in rat cardiac myocytes. *Biochem Biophys Res Commun* 2007;**353**:67-73.
- Potthoff M-J, Olson E-N. *MEF2*: a central regulator of diverse developmental programs. *Development* 2007;**134**:4131-4140.
- Arnold M-A, Kim Y, Czubryt M-P, Phan D, McAnally J, Qi X *et al*. *MEF2C* transcription factor controls chondrocyte hypertrophy and bone development. *Dev Cell* 2007;**12**:377-389.
- Li X-G, Okada T, Kadera M, Nara Y, Takino N, Muramatsu C *et al*. Viral-mediated temporally controlled dopamine production in a rat model of Parkinson disease. *Mol Ther* 2006;**13**:160-166.
- Kuwahara K, Teg Pipes G-C, McAnally J, Richardson J-A, Hill J-A, Bassel-Duby R *et al*. Modulation of adverse cardiac remodeling by STARS, a mediator of *MEF2* signaling and SRF activity. *J Clin Invest* 2007;**117**:1324-1334.
- Pachucki J, Burmeister LA, Larsen PR. Thyroid hormone regulates hyperpolarization-activated cyclic nucleotide-gated channel (HCN2) mRNA in the rat heart. *Circ Res* 1999;**85**:498-503.
- Yanagi K, Takano M, Narazaki G, Uosaki H, Hoshino T, Ishii T *et al*. HCN and Cav3 channels confer automaticity of embryonic stem-derived cardiomyocytes. *Stem Cells* 2007;**25**:2712-2719.
- Jochum W, Passegue E, Wagner EF. AP-1 in mouse development and tumorigenesis. *Oncogene* 2001;**20**:2401-2412.
- Lin Q, Schwarz J, Bucana C, Olson E-N. Control of mouse cardiac morphogenesis and myogenesis by transcription factor *MEF2C*. *Science* 1997;**276**:1404-1407.
- Kim Y, Phan D, van Rooij E, Wang D-Z, McAnally J, Qi X *et al*. The *MEF2D* transcription factor mediates stress-dependent cardiac remodeling in mice. *J Clin Invest* 2008;**118**:124-132.
- Naya F-J, Black B-L, Wu H, Bassel-Duby R, Richardson J-A, Hill J-A *et al*. Mitochondrial deficiency and cardiac sudden death in mice lacking *MEF2A* transcription factor. *Nat Med* 2002;**11**:1303-1309.
- Zhao X-S, Gallardo T-D, Lin L, Schageman J-J, Shohet R-V. Transcriptional mapping and genomic analysis of the cardiac atria and ventricles. *Physiol Genomics* 2002;**12**:53-60.

Self-Contained Induction of Neurons from Human Embryonic Stem Cells

Tsuyoshi Okuno^{1,2}, Takashi Nakayama³, Nae Konishi¹, Hideo Michibata¹, Koji Wakimoto¹, Yutaka Suzuki¹, Shinji Nito¹, Toshio Inaba², Imaharu Nakano⁴, Shin-ichi Muramatsu⁴, Makoto Takano⁵, Yasushi Kondo^{1*}, Nobuo Inoue⁶

1 Advanced Medical Research Laboratory, Mitsubishi Tanabe Pharma Corporation, Osaka, Japan, **2** Department of Advanced Pathobiology, Graduate School of Life and Environmental Sciences, Osaka Prefecture University, Osaka, Japan, **3** Department of Biochemistry, Yokohama City University School of Medicine, Yokohama, Japan, **4** Division of Neurology, Department of Medicine, Jichi Medical University, Tochigi, Japan, **5** Department of Physiology, Jichi Medical University, Tochigi, Japan, **6** Laboratory of Regenerative Neurosciences, Graduate School of Human Health Sciences, Tokyo Metropolitan University, Tokyo, Japan

Abstract

Background: Neurons and glial cells can be efficiently induced from mouse embryonic stem (ES) cells in a conditioned medium collected from rat primary-cultured astrocytes (P-ACM). However, the use of rodent primary cells for clinical applications may be hampered by limited supply and risk of contamination with xeno-proteins.

Methodology/Principal Findings: We have developed an alternative method for unimpeded production of human neurons under xeno-free conditions. Initially, neural stem cells in sphere-like clusters were induced from human ES (hES) cells after being cultured in P-ACM under free-floating conditions. The resultant neural stem cells could circumferentially proliferate under subsequent adhesive culture, and selectively differentiate into neurons or astrocytes by changing the medium to P-ACM or G5, respectively. These hES cell-derived neurons and astrocytes could procure functions similar to those of primary cells. Interestingly, a conditioned medium obtained from the hES cell-derived astrocytes (ES-ACM) could successfully be used to substitute P-ACM for induction of neurons. Neurons made by this method could survive in mice brain after xeno-transplantation.

Conclusion/Significance: By inducing astrocytes from hES cells in a chemically defined medium, we could produce human neurons without the use of P-ACM. This self-serving method provides an unlimited source of human neural cells and may facilitate clinical applications of hES cells for neurological diseases.

Citation: Okuno T, Nakayama T, Konishi N, Michibata H, Wakimoto K, et al. (2009) Self-Contained Induction of Neurons from Human Embryonic Stem Cells. PLoS ONE 4(7): e6318. doi:10.1371/journal.pone.0006318

Editor: Tailoi Chan-Ling, University of Sydney, Australia

Received: June 3, 2008; **Accepted:** June 24, 2009; **Published:** July 21, 2009

Copyright: © 2009 Okuno et al. This is an open-access article distributed under the terms of the Creative Commons Attribution License, which permits unrestricted use, distribution, and reproduction in any medium, provided the original author and source are credited.

Funding: Part of this work was supported by grants from the Ministry of Education, Science, Sports and Culture, the Japanese Government; and from the Japan Ministry of Health, Labor and Welfare.

Competing Interests: The authors have declared that no competing interests exist.

* E-mail: kondo.yasushi@mc.mt-pharma.co.jp

Introduction

Embryonic stem (ES) cells, derived from the inner cell mass of blastocysts, are pluripotent cells that can differentiate into a variety of cell types including neural cells [1,2]. Among the various basic and clinical applications for ES cells, cell transplantation therapy for central nervous diseases is of particular interest because differentiated neurons do not proliferate, and a relatively large number of donor cells are necessary to replace diseased neurons. Several methods have been developed to prepare neural cells from ES cells. Neurons can be obtained indirectly from ES cells via ectodermal cells in embryoid bodies, which are formed from dissociated ES cells, either by induction with retinoic acid or selection [3,4]. Alternatively, neural stem cells and neurons can be directly differentiated from ES cells without forming embryoid bodies by culturing ES cells on mouse-cultured stroma cells (PA-6) [5], or under chemically defined low-density culture conditions [6]. All of these procedures, however, are time consuming and require highly complicated processes to

generate many neurons. In addition, their practicality is limited by the possible teratogenicity caused by culture factors, such as retinoic acid, of differentiated cells. We have previously reported an efficient method to prepare transplantable neural cells from mouse ES cells using a conditioned medium collected from rat primary-cultured astrocytes (P-ACM) [7–9]. In this study, we applied this method to human ES (hES) cells for induction of neurons and astrocytes. Once the astrocytes were derived from hES cells, they could be substituted for primary astrocytes that induce neurons, thus achieving xeno-free production of neurons.

Results

Neural cell differentiation from hES

Four hES cell-lines stably expressing humanized renilla green fluorescent protein (hrGFP) were obtained. These hES cell-lines were kept in undifferentiated state with positive stem cell markers, such as alkaline phosphatase, Oct-4, and SSEA-4. When cultured

in P-ACM containing fibroblast growth factor-2 (FGF-2) under free-floating conditions, colonies of undifferentiated hES cells gave rise to floating spheres composed of neural stem cells and undifferentiated cells, which gradually increased in size during the culture. After 12 days of culture, the spheres were plated onto a poly-L-Lysine/Laminin coated dish and cultivated in neural stem cell medium (NSCM) containing high concentrations of FGF-2 and epidermal growth factor (EGF). Within 24 h, the spheres attached onto the substrate and formed circular clusters of cells. Many of these cells subsequently migrated to the surrounding areas and covered the growth surface of the dish in circular monolayers. After replacing NSCM by P-ACM and culture for 14 days, the spheres differentiated into neurons (Figures 1A, B) and few astrocytes (Figures 1C). These were identified by the neuronal marker tubulin β III isoform (Tuj1) and the astrocytic marker glial fibrillary acidic protein (GFAP).

Selective differentiation of hES cells into neurons and astrocytes

By culture of the spheres in NSCM, neural stem cells were able to migrate from the attached spheres to the surrounding area and subsequently form a circular cluster. NSCM containing FGF-2 and EGF promotes neural stem cells proliferation, while repressing their differentiation into any type of neural cells. After removing the core of the attached spheres mechanically, the remaining neural stem cells could proliferate in NSCM and selectively differentiate into neurons and astrocytes by subculture in an appropriate medium. To differentiate into neurons, neural stem cells were subcultured using 0.05% Trypsin/EDTA in P-ACM for 14 days (Figures 2A, B). After these 14 days of subculture, a large number of cells expressed Tuj1 ($84.0 \pm 5.1\%$, $n = 3$). On the other hand, to differentiate into astrocytes, neural stem cells were subcultured in G5 medium for 14 days (Figure 2C). After this subculture, a large number of cells expressed

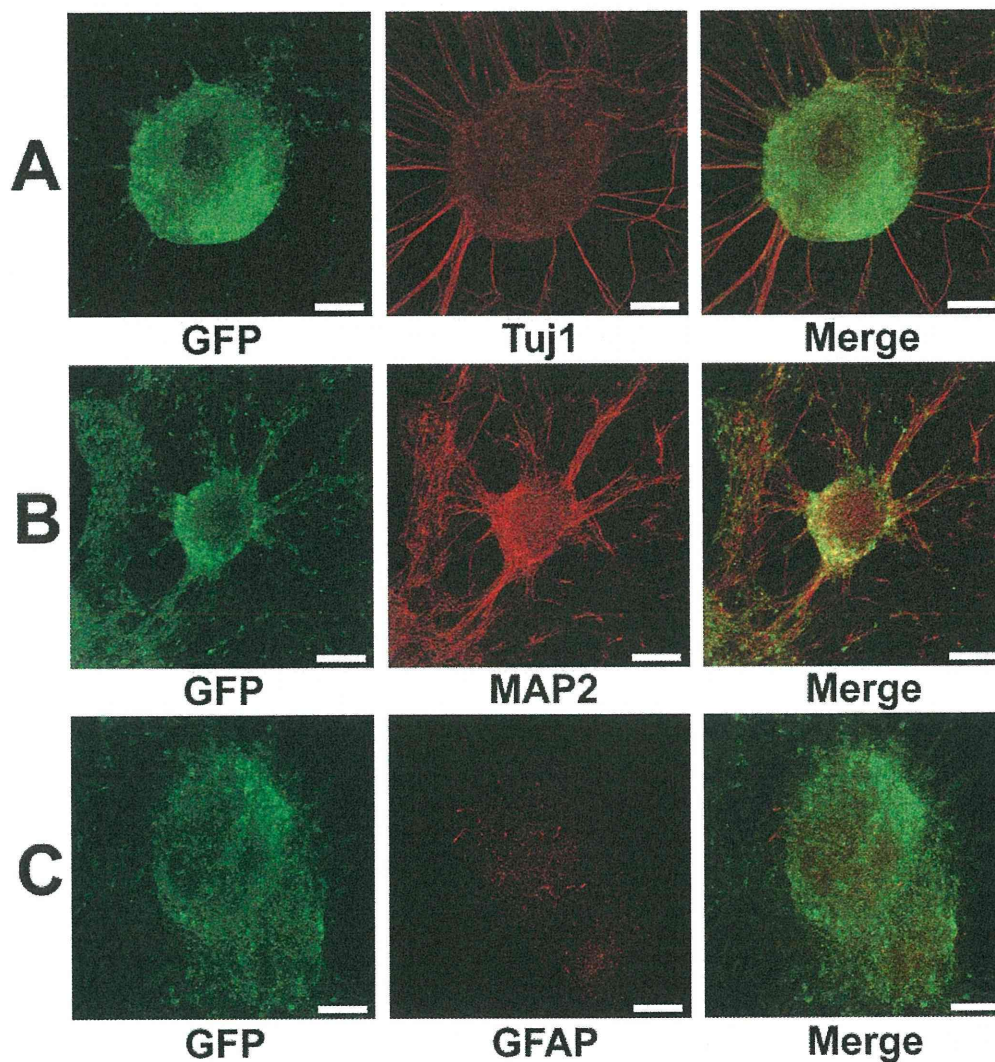


Figure 1. Differentiation of hES cells into neurons in P-ACM. Floating spheres composed of neural stem cells and undifferentiated cells grown for 12 days were plated on an adhesive substrate and cultured for 14 days in P-ACM. Expression of hrGFP (green), Tuj1 (A, red), MAP2 (B, red), and GFAP (C, red) staining of the many neural and few glial cells derived from hES cells. Bar = 100 μ m. doi:10.1371/journal.pone.0006318.g001

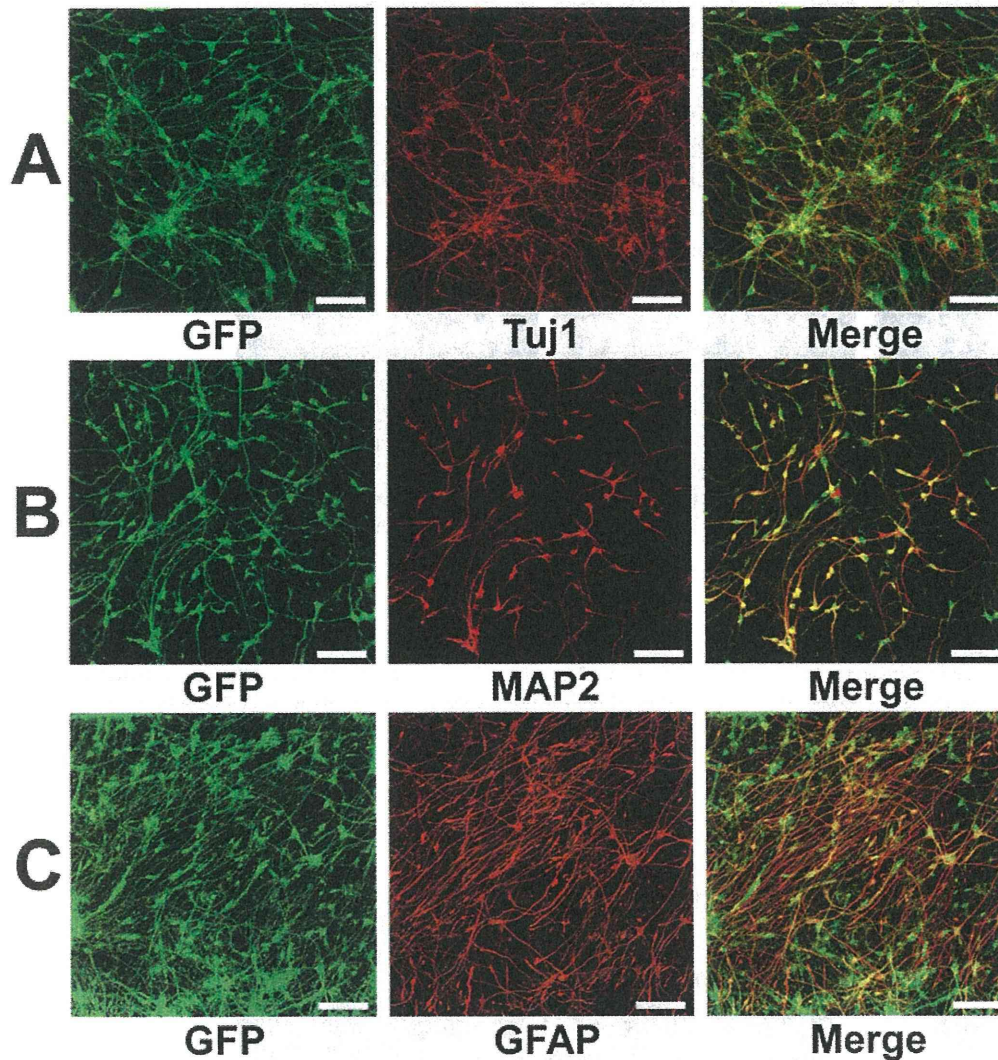


Figure 2. Selective induction of hES cells into neurons and astrocytes. (A, B): Neural stem cells that had migrated from floating spheres in NSCM were subcultured onto a PLL coated plate and cultured for 14 days in P-ACM. Immunostaining with antibody to Tuj1 and MAP2 showed that the subcultured neural stem cells had differentiated into neurons. Expression of hrGFP (green), (A) Tuj1 (red), and (B) MAP2 (red) staining profiles. (C): Neural stem cells were cultured for 14 days after removal of the core of spheres with a glass pipette and change of medium to G5 medium. The proliferated cells were subcultured onto PLL/LAM coated plate and cultured for 14 days in G5 medium. Immunostaining with antibody to GFAP showed that the subcultured cells had differentiated into astrocytes. Expression of hrGFP (green) and GFAP (red) staining profiles. Bar=100 μ m. doi:10.1371/journal.pone.0006318.g002

GFAP ($75.0 \pm 1.2\%$, $n = 3$). The removed core of the attached spheres could, like the first spheres, be used repeatedly (about twenty times) as seed for neural stem cells.

Xeno-free induction of astrocytes using a chemically defined medium

For collection of xeno-free astrocytes derived from hES cells, we used a chemically defined N2 medium for neural induction. When cultured in N2 medium containing FGF-2 and EGF under free-floating conditions, colonies of undifferentiated hES cells gave rise to floating spheres. As N2 was less efficient than P-ACM for obtaining astrocytes, we prepared hES cells in large scale ($>10^8$ cells). After differentiation, millions of astrocytes were gained under xeno-free condition (Figure 3A).

Neuronal induction of hES cell-derived astrocytes

Next, we investigated whether the astrocytes derived from hES cells can be substituted for primary astrocytes to differentiate hES cells into neural cells. A conditioned medium of hES cell-derived astrocytes was collected after two days culture and used as ES-ACM by adding an equal amount of N2 medium. As in the case of P-ACM, hES cells cultured in ES-ACM differentiated into neural cells via formation of spheres. After switching the cells from NSCM to ES-ACM, many cells had neuronal-like appearance with long neurites. By 6 weeks of culture in ES-ACM, most cells had neural morphology and expressed microtubule-associated protein 2 (MAP2) (Figure 3B). During our procedure for differentiating hES cells using ES-ACM, expression of several markers was analyzed by RT-PCR (Figure 4A). By 8 weeks culture

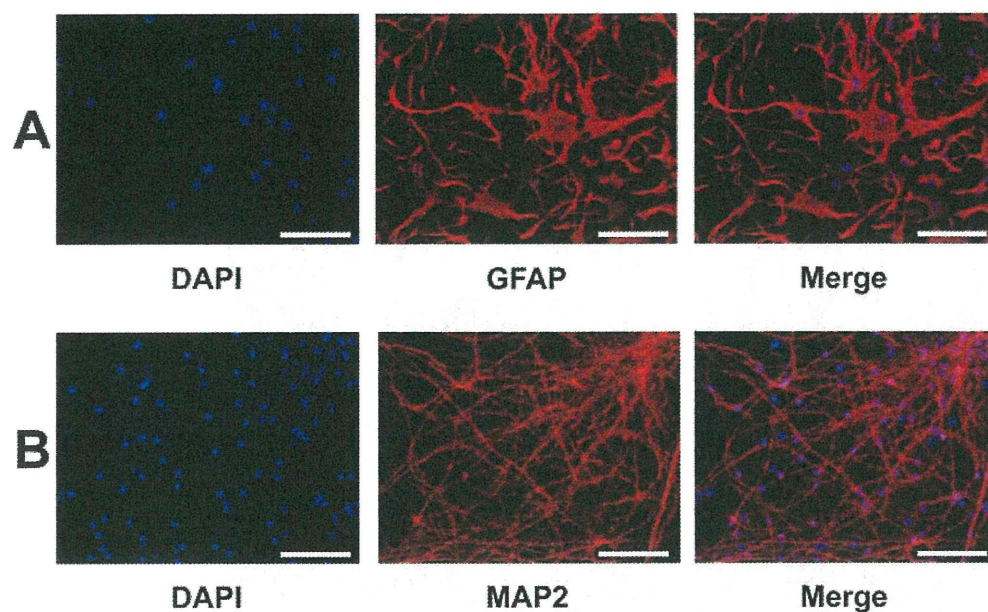


Figure 3. Differentiation of hES cells into astrocytes in a chemically defined medium. (A): Neural stem cells induced by N2 medium were cultured for 14 days after removal of the core of spheres with a glass pipette and change of medium to G5 medium. The proliferated cells were subcultured onto a PLL/LAM coated plate and cultured for 14 days in G5 medium. Immunostaining with antibody to GFAP showed that most of the subcultured cells had differentiated into astrocytes. DAPI (blue) and GFAP (green) staining profiles. Neural stem cells induced by xeno-free ES-ACM were subcultured onto PLL coated plate and cultured for 6 weeks in ES-ACM. (B): Immunostaining with antibody to MAP2 showed that the subcultured NSCs had differentiated into mature neurons. DAPI (blue) and MAP2 (red) staining profiles. Bar = 100 μ m. doi:10.1371/journal.pone.0006318.g003

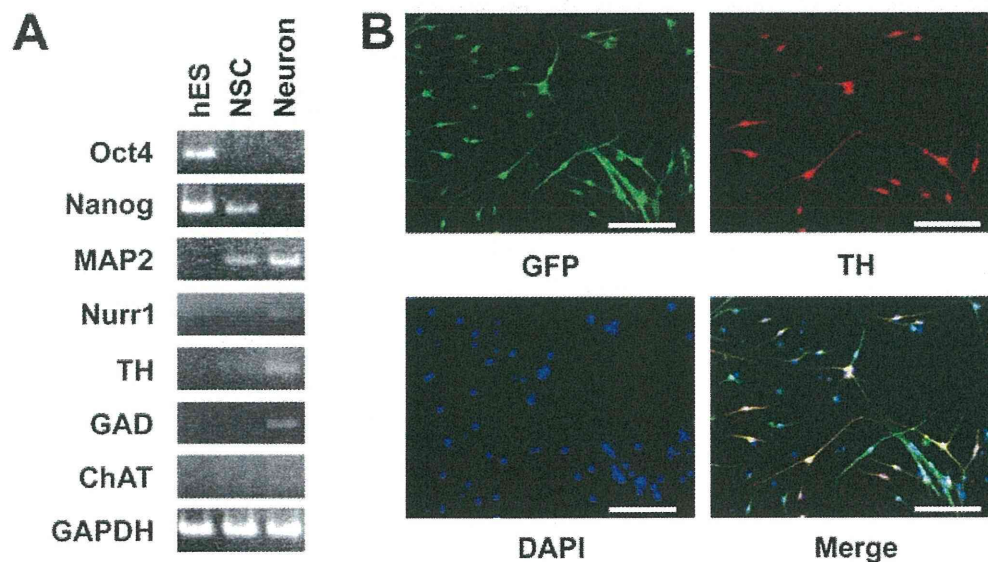


Figure 4. RT-PCR analysis and differentiation of hES cells into dopaminergic neurons in xeno-free ES-ACM. (A): RT-PCR analysis of hES cells, neural stem cells and mature neurons. RNA was isolated from clones of undifferentiated hES cells, from neural stem cells, and from mature neurons which had been cultured for 8 weeks in ES-ACM and analyzed for expression of marker genes. The expression levels of each gene were normalized to GAPDH gene expression level. hES, undifferentiated hES cells; NSC, neural stem cells; Neuron; mature neurons. (B): Differentiation of hES cells into dopaminergic neural cells in xeno-free ES-ACM. Neural stem cells induced by ES-ACM were subcultured onto PLL coated plate and cultured for 8 weeks in ES-ACM. Immunostaining with antibody TH and expression of hrGFP showed that the subcultured neural stem cells had differentiated into dopaminergic neurons. Expression of hrGFP (green), DAPI (blue) and TH (red) staining profiles. Bar = 100 μ m. doi:10.1371/journal.pone.0006318.g004

in ES-ACM, some cells showed tyrosine hydroxylase (TH) - immunoreactivity (Figure 4B). Furthermore, when cultured in ES-ACM again, the cells could differentiate into astrocytes via formation of spheres. To induce differentiation of neural stem cells into astrocytes, the culture medium was changed from NSCM to G5 medium. After medium change, most neural stem cells had the appearance of typical astrocytes. By 2 weeks culture in G5 medium, the majority ($82.4 \pm 1.8\%$, $n = 3$) of cells expressed GFAP, and few ($<1\%$) expressed MAP2.

Electrophysiological analysis of neurons differentiated from hES cells

For electrophysiological study, hES-derived neurons were cultured on coverslips for 4–6 weeks. The coverslips were transferred to a recording chamber before use. Neurons were selected based on their appearance (spherical shape with long neurites). The resting membrane potential of the neurons were $-62.0 \sim -11.1$ mV ($n = 26$). Among 26 cells examined, action potentials were elicited in 22 cells (Figure 5A, Control). Application of $1 \mu\text{M}$ tetrodotoxin (TTX) completely suppressed the overshoot (Figure 5A, right panel). The action potentials were evoked only when resting membrane potentials were set to -70 mV by current injection in 11 cells. The rest of the cells did not possess membrane excitability ($n = 4$ out of 26, closed circle in Figure 5B).

Survival of hES cell-derived neurons in mice brain

To examine differentiation of hES cell-derived cells *in vivo*, we transplanted neural stem cells induced with ES-ACM into mice brain ($n = 7$). Before transplantation, the majority ($85.1 \pm 5.1\%$, $n = 4$) of donor cells expressed Nestin, a marker for neural stem cell (Figure 6A), and no cells expressed octamer transcription factor-3 (Oct-3) and stage-specific embryonic antigen (SSEA-4), two makers for undifferentiated cells (data not shown). Four weeks after engraftment, many ($2\text{--}3 \times 10^3$) hrGFP-positive cells were recognized (Figure 6B, C). Some of these cells ($<10\%$) were also Tuj1-immunoreactive (Figure 6D). In the vicinity of the grafts, few cells were immunoreactive against Ki-67, a marker for proliferation. However, none of these Ki-67-positive cells were positive for hrGFP (Figure 6E). Teratoma was not detected in any of the transplanted mice.

Discussion

We have shown in this study that neurons and astrocytes can be produced efficiently from hES cells using a conditioned medium collected from either rat primary-cultured astrocytes or hES cell-derived astrocytes. Astrocytes derived from hES cells can be used for continuous generation of neurons. Although a number of media including serum-free media supplemented with various cytokines and/or growth factors have been developed [10,11] to keep a long-term culture of neuronal cells, synthetic culture systems can usually maintain neural cells stable for only few weeks. Although a conditioned medium of primary-cultured astrocytes can be effective in culturing neurons for a longer period of time, the use of primary astrocytes may not be practical due to a number of limitations, including restricted availability of neural tissues as source of astrocytes, and extensive time and effort to obtain astrocytes from living tissues. Additionally, it is very difficult to maintain a stable culture of primary cells in a culture vessel, and subculture of these cells is limited within few passages.

The properties of primary-cultured astrocytes vary depending on the maturation stage of the living body and the region of the living tissue from which the astrocytes are derived. In addition,

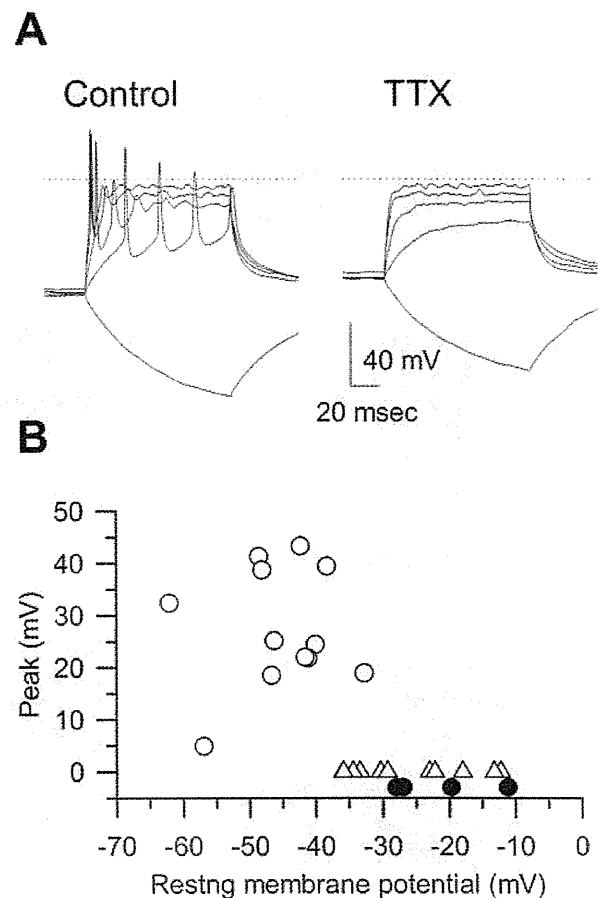


Figure 5. Electrophysiological properties of hES-derived neurons. (A): (Control) Action potentials elicited by depolarizing current injections (50 pA steps for 100 msec). The resting membrane potential was -62.0 mV. During the hyperpolarizing pulse (-50 pA), no 'sag' component was observed. (TTX) Membrane potentials recorded in the presence of $1 \mu\text{M}$ tetrodotoxin. In both panels, the dotted lines indicate 0 mV. (B): Summary of the resting membrane potentials and the peak amplitudes. Open circle; cells with action potentials. Open triangle; cells with action potentials only when the resting membrane potential was set to -70 mV. Closed circle; cells without membrane excitability. doi:10.1371/journal.pone.0006318.g005

when astrocytes are obtained from a living body, contamination with cells other than the desired astrocytes is inevitable. Thus, it is difficult to prepare a stable astrocyte-conditioned medium having substantially uniform quality. With our method, on the other hand, ES-ACM can efficiently induce differentiation of hES cells into neural cells. Moreover, large amounts of ES-ACM can be produced stably and readily. ES-ACM, like P-ACM, can keep neuron cultures stable for more than eight weeks until mature neuronal phenotypes are apparent. In addition, completely xeno-free ES-ACM can be generated from immature hES cells by culture in chemically defined medium. With this completely xeno-free ES-ACM, xeno-free neurons and astrocytes can repeatedly be produced. In our transplantation experiment, donor cells did not express undifferentiated markers, such as Oct-3 and SSEA-4. In addition, only few Ki-67 positive cells found in the vicinity of the grafts were hrGFP-negative. These cells were unlikely to be derived from donor cells. It is important to exclude tumorigenicity of neuronal cells derived with this xeno-free method in future

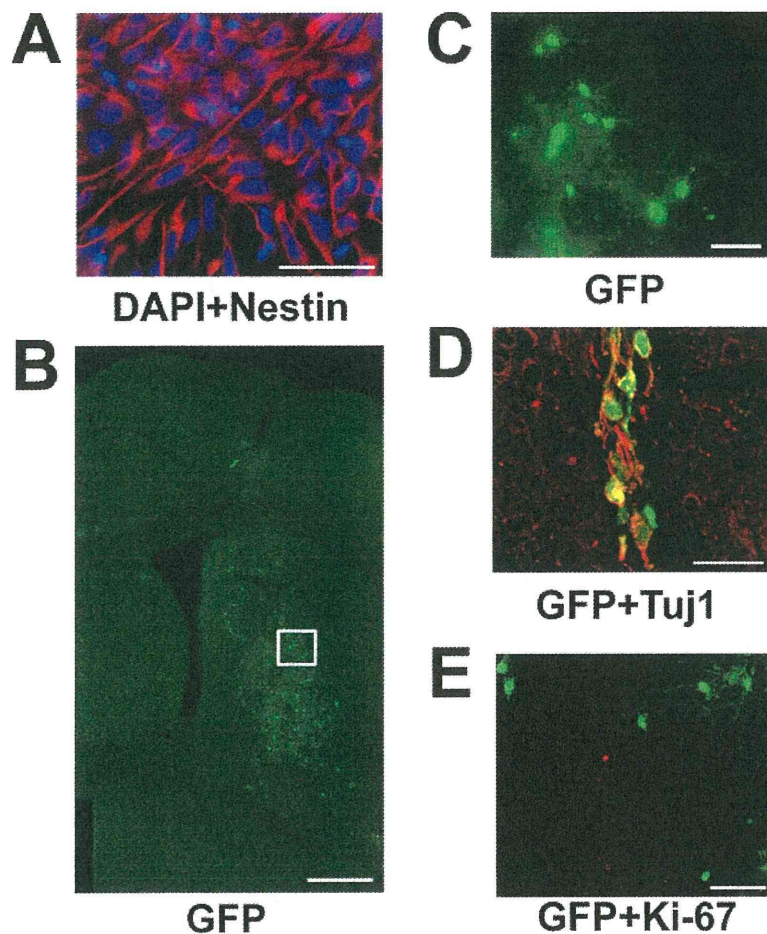


Figure 6. Survival of transplanted neural stem cells *in vivo*. (A): Most of the donor cells were confirmed to be Nestin-immunoreactive neural stem cells before transplantation. Anti-Nestin staining (green) and DAPI (blue). Bar = 50 μ m. (B): Transplantation site. Grafted cells expressing hrGFP can be seen in the striatum. Bar = 500 μ m. (C): High power magnification view of a white box in panel A. Some of the hrGFP-positive cells display a morphology similar to that of neurons. Bar = 50 μ m. (D): Merged image of hrGFP expression (green) and immunostaining of anti-Tuj1 (red). Bar = 20 μ m. (E): Merged image of hrGFP expression (green) and immunostaining of anti-Ki-67 (red). Bar = 50 μ m.
doi:10.1371/journal.pone.0006318.g006

study for application to the cell therapy. Further studies are necessary to identify the specific molecules that induce neural cells in P- and ES-ACMs.

Recently, two methods adopting human tissue-derived cells have been reported as appropriate for clinical applications. One is an improved stromal cell-induced method that uses an amniotic membrane matrix [12]. The other uses telomerase-immortalized midbrain astrocytes [13]. Although both methods are xeno-free, they still need primary human tissues. On the other hand, with our method, neural cells can be induced from ES cells themselves. This self-serving method can supply donor cells consistently and may have an advantage for clinical applications.

Materials and Methods

ES cell culture

All experiments using hES cells were performed in conformity with “The Guidelines for Derivation and Utilization of Human Embryonic Stem Cells” of the Japanese government after approval by the institutional review board of Mitsubishi Tanabe Pharma Corporation. Two hES cell lines, SA002 and SA181, were obtained

from Cellartis AB (Goteborg, Sweden) [14] and maintained on a mitotically inactivated mouse embryonic fibroblast feeder layer in a culture medium (vitroHES, Vitrolife AB, Goteborg, Sweden), supplemented with 4 ng/ml FGF-2 (Invitrogen, Carlsbad, CA). For passaging, the hES cells were treated with collagenase type IV (200 U/ml; Invitrogen) for 5 min, gently scraped from the culture dish, and then split 1:2–1:4 onto a feeder layer of mouse embryonic fibroblasts inactivated with 10 μ g/ml mitomycin C.

Electroporation

All recombinant DNA experiments conformed to National Institute of Health (NIH) guidelines. First, a pGFP plasmid, in which hrGFP (Stratagene, La Jolla, CA) was expressed under the control of a CAG promoter (a gift from J. Miyazaki) [15] was constructed. Ten micrograms of the linearized plasmid was then electroporated into a suspension of hES cells (10^7 cells) in 0.8 mL of PBS using a Gene Pulser (500 μ F, 250 V, Bio-Rad, Hercules, CA). The cells were next incubated on ice for 10 minutes, plated, and allowed to recover for 24 hours before selection with G418 (200 μ g/mL). The cells were daily fed with the culture medium containing G418 for 12 days, after which the resulting ten G418-

resistant ES colonies showing strong hrGFP expression were individually picked and propagated. To analyze stem cell markers, alkaline phosphatase activity and cell surface markers were detected using an ES cell characterization kit (Chemicon, Temecula).

hES cell differentiation

Whole colonies of undifferentiated hES cells, 800–1000 μm in diameter, were picked up from the feeder layer using a glass capillary and transferred into non-adhesive bacteriological dishes each containing P-ACM supplemented with 20 ng/ml FGF-2 (R&D Systems Inc., Minneapolis). P-ACM was prepared as described previously [7]. The colonies were then cultured for 12 days, giving rise to spheres, which were next plated onto poly-L-Lysine/Laminin (Sigma-Aldrich, St. Louis) coated dishes and cultivated for seven days in NSCM (Neurobasal medium supplied with B27 supplement, both from Invitrogen, 20 ng/ml FGF-2, and 20 ng/ml recombinant EGF [R&D systems]). At this stage, the spheres gave rise to circular clusters of cells, many of which migrated to the clusters to the surrounding areas. After replacing the NSCM with P-ACM and culture for 14 days, the spheres differentiated into neurons and few astrocytes. To obtain more and purer neurons, the centers of the clusters containing undifferentiated ES cells were removed with a glass capillary, and the rest of the clusters were cultured for seven days in NSCM. Neuronal differentiation was then induced by subculture of neural stem cells using 0.05% Trypsin/EDTA in P-ACM for 14 days. To induce astrocytic differentiation, the neural stem cells were subcultured in G5 medium (Neurobasal medium supplemented with G5 supplement, both from Invitrogen, 10 ng/ml FGF-2, and 20 ng/ml EGF) for 14 days.

To induce astrocytic differentiation under xeno-free conditions, the colonies of hES cells were transferred into non-adhesive bacteriological dishes each containing N2 medium (Neurobasal medium supplied with N2 supplement, Invitrogen) supplemented with 20 ng/ml of FGF-2 and EGF. After the colonies were cultured for 12 days, few of them gave rise to spheres containing neural stem cells, which were subsequently plated onto poly-L-Lysine/Laminin in G5 medium. Centers of the spheres containing undifferentiated hES cells were removed with a glass capillary, and the rest of the clusters were cultured for seven days in G5 medium. By repeating over this cycle eight times, the spheres were purified to obtain pure neural stem cells. These neural stem cells were subcultured in G5 medium for 14 days to induce astrocytes. For collection of ES-ACM, hES cells derived-astrocytes were cultured in N2 medium for two days.

Immunostaining analysis

hES cells cultured in a 24-well plate were fixed in 4% paraformaldehyde in phosphate-buffered saline (PBS). Immunocytochemistry was performed using standard protocols and antibodies directed against Tuj1 (monoclonal 1:1000), MAP2 (monoclonal, 1:1000), GFAP (polyclonal 1:500), Oct-4 (monoclonal 1:500), SSEA-4 (monoclonal 1:400), Nestin (monoclonal 1:1000) (all from Chemicon), and TH (monoclonal, 1:400) (Acris Antibodies, Hiddenhausen, Germany). Alexa Fluor 594-labeled (Molecular Probes, Eugene, OR) and Cy3-labeled (GE healthcare, Uppsala, Sweden) secondary antibodies were used for visualization. 4', 6-diamidino-2-phenylindole (DAPI, Kirkegaard Perry Laboratories, Gaithersburg) was used for nuclei staining.

Cell density of neural lineages (neurons and astrocytes) was determined by counting the numbers of DAPI, Tuj1⁺ and GFAP⁺ cells per field at a magnification of 200 times using an inverted microscope. Five visual fields were randomly selected and counted

for each sample. Numbers presented in figures represent the average percentage and SEM of positive cells over DAPI from three samples per each examination.

RT-PCR analysis

Total RNA was extracted from undifferentiated hES cells, neural stem cells, and neuronal cells using QIAshredder (QIAGEN, Hilden, Germany) and RNeasy Plus Mini kit (QIAGEN). Reverse transcription was carried out using random hexamers at 37°C for 60 minutes according to the manufacturer's instruction for First-Strand cDNA Synthesis Kit (GE Healthcare UK Ltd., Buckinghamshire, UK). PCR was carried out for 30 cycles using the specific primer sets. The reaction cycle was set at 95°C for 30 seconds, 55°C for 30 seconds, and 72°C for 30 seconds. The amplified fragments were subjected to electrophoresis in a 2% agarose gel, which was subsequently stained with ethidium bromide and photographed. The primers used are as follows: glyceraldehyde-3-phosphatedehydrogenase (GAPDH), ACCA-CAGTCCATGCCATCAC and TCCACCACCCTGTTGCTG-TA; Oct4, CGTTCCTTTGGAAGGTGTTC and ACACT-CGGACCACGTCTTTC; Nanog, AAGACAAGGTCCCGGT-CAAG and CCTAGTGGTCTGCTGTATTAC; MAP2, CTTT-CCGTTTCATCTGCCATT and GCATATGCGCTGATTCT-TCA; Nurr1, GCTAAACAAAACCTTGCATGC and CTCATATCATGTGCCATACTAG; TH, GAGTACACCGCCGAG-GAGATTG and GCGGATATACTGGGTGCACTGG; choline acetyltransferase (ChAT), ATGGGGCTGAGGACAGCGAAG and AAGTGTGCGATGCACTGCAGG; glutamic acid decarboxylase (GAD), ATTCTTGAAGCCAAACAG and TAGCTT-TTCCCCTCGTTG.

Electrophysiology

The action potential was recorded using current clamp mode of Axopatch200B amplifier and Digidata 1320 interface (Axon, CA, USA). Physiological bathing solution contained (in mM); 140 NaCl, 5.4 KCl, 0.33 NaH₂PO₄, 0.5 MgCl₂, 1.8 CaCl₂, 5 HEPES (pH = 7.4 with NaOH). Standard high K⁺ pipette solution contained; 110 Aspartic acid, 30 KCl, 5 MgATP, 5 Na₂ creatine phosphate, 0.1 Na₂GTP, 2 EGTA, 10 HEPES (pH = 7.2 with KOH). Electrode resistance was 8–6 MOhm. All experiments were carried out at 33–35°C.

Transplantation Experiment

Neural stem cells derived from hES cells using ES-ACM were implanted into the mouse striatum. All animal experimental protocols were approved by the Animal Ethics Committee of Mitsubishi Tanabe Pharma Corporation. 8-week-old C57BL/6 Cr Slc mice (SLC, Shizuoka, Japan) were anesthetized with pentobarbital and fixed on a stereotactic device (Narishige, Tokyo, Japan). By using a glass pipette with an inner diameter of 100 μm , 1×10^5 cells/5 μl were slowly (0.3 $\mu\text{l}/\text{min}$) injected into the striatum (AP \pm 0 mm, ML +2.0 mm, DV –3.0 mm from bregma) of an adult male mouse. Four weeks after the transplantation, the recipient mouse was anesthetized with pentobarbital and perfused with ice-cold 4% paraformaldehyde in PBS. The brains of each mouse were postfixed in the same solution, cryoprotected with 30% sucrose in PBS for 48 h, and frozen. Coronal sections (thickness 40 μm) were cut on a microtome with freezing unit, collected in PBS (pH 7.4), and divided into series. Brain sections were incubated overnight with primary antibodies at 4°C. The primary antibodies used for immunohistochemistry were mouse anti-Tuj1 (1:800, Covance, USA) and rabbit anti-Ki67 (1:25, abcam, UK). For detection of the primary antibodies, Alexa Fluor 594 goat anti-mouse IgG (1:1000; Molecular Probes) and Alexa

Fluor 594 goat anti-rabbit IgG (1:1000; Molecular Probes) were incubated with the samples. Immunoreactivity was assessed and viewed under confocal laser scanning microscopy (FV10i; Olympus, Tokyo).

Acknowledgements

We thank Jun-ichi Miyazaki, Osaka University Medical School, Osaka, Japan for the generous gift of plasmid pCAG. We also thank Naomi Takino and Hiroko Nishida, Division of Neurology, Department of

Medicine, Jichi Medical University, Tochigi, Japan, for their technical assistance.

Author Contributions

Conceived and designed the experiments: TO HM SiM YK. Performed the experiments: TO NK HM KW MT. Analyzed the data: TO HM YS SN TI IN SiM MT YK. Contributed reagents/materials/analysis tools: TN SiM MT NI. Wrote the paper: TO SiM MT YK.

References

1. Thomson JA, Itskovitz-Eldor J, Shapiro SS, Waknitz MA, Swiergiel JJ, et al. (1998) Embryonic stem cell lines derived from human blastocysts. *Science* 282: 1145–1147.
2. Suemori H, Tada T, Torii R, Hosoi Y, Kobayashi K, et al. (2001) Establishment of embryonic stem cell lines from cynomolgus monkey blastocysts produced by IVF or ICSI. *Dev Dyn* 222: 273–279.
3. Bain G, Kitchens D, Yao M, Huettner JE, Gottlieb DI (1995) Embryonic stem cells express neuronal properties in vitro. *Dev Biol* 168: 342–357.
4. Okabe S, Forsberg-Nilsson K, Spiro AC, Segal M, McKay RD (1996) Development of neuronal precursor cells and functional postmitotic neurons from embryonic stem cells in vitro. *Mech Dev* 59: 89–102.
5. Kawasaki H, Mizuseki K, Nishikawa S, Kaneko S, Kuwana Y, et al. (2000) Induction of midbrain dopaminergic neurons from ES cells by stromal cell-derived inducing activity. *Neuron* 28: 31–40.
6. Tropepe V, Hitoshi S, Sirard C, Mak TW, Rossant J, et al. (2001) Direct neural fate specification from embryonic stem cells: a primitive mammalian neural stem cell stage acquired through a default mechanism. *Neuron* 30: 65–78.
7. Nakayama T, Momoki-Soga T, Inoue N (2003) Astrocyte-derived factors instruct differentiation of embryonic stem cells into neurons. *Neurosci Res* 46: 241–249.
8. Nakayama T, Momoki-Soga T, Yamaguchi K, Inoue N (2004) Efficient production of neural stem cells and neurons from embryonic stem cells. *Neuroreport* 15: 487–491.
9. Nakayama T, Sai T, Otsu M, Momoki-Soga T, Inoue N (2006) Astrocytogenesis of embryonic stem-cell-derived neural stem cells: Default differentiation. *Neuroreport* 17: 1519–1523.
10. Bottenstein JE, Sato GH (1979) Growth of a rat neuroblastoma cell line in serum-free supplemented medium. *Proc Natl Acad Sci U S A* 76: 514–517.
11. Brewer GJ, Cotman CW (1989) Survival and growth of hippocampal neurons in defined medium at low density: advantages of a sandwich culture technique or low oxygen. *Brain Res* 494: 65–74.
12. Ueno M, Matsumura M, Watanabe K, Nakamura T, Osakada F, et al. (2006) Neural conversion of ES cells by an inductive activity on human amniotic membrane matrix. *Proc Natl Acad Sci U S A* 103: 9554–9559.
13. Roy NS, Cleren C, Singh SK, Yang L, Beal MF, et al. (2006) Functional engraftment of human ES cell-derived dopaminergic neurons enriched by coculture with telomerase-immortalized midbrain astrocytes. *Nat Med* 12: 1259–1268.
14. Heins N, Englund MC, Sjöblom C, Dahl U, Tønning A, et al. (2004) Derivation, characterization, and differentiation of human embryonic stem cells. *Stem Cells* 22: 367–376.
15. Niwa H, Yamamura K, Miyazaki J (1991) Efficient selection for high-expression transfectants with a novel eukaryotic vector. *Gene* 108: 193–199.

Nurr1 Is Required for Maintenance of Maturing and Adult Midbrain Dopamine Neurons

Banafsheh Kadkhodaei,¹ Takehito Ito,² Eliza Joodmardi,¹ Bengt Mattsson,³ Claude Rouillard,¹ Manolo Carta,³ Shin-Ichi Muramatsu,⁴ Chiho Sumi-Ichinose,⁵ Takahide Nomura,⁵ Daniel Metzger,⁶ Pierre Chambon,⁶ Eva Lindqvist,⁷ Nils-Göran Larsson,^{8,10} Lars Olson,⁷ Anders Björklund,³ Hiroshi Ichinose,² and Thomas Perlmann^{1,9}

¹Ludwig Institute for Cancer Research, Stockholm Branch, SE-171 77 Stockholm, Sweden, ²Graduate School of Bioscience and Biotechnology, Tokyo Institute of Technology, Yokohama 226-8501, Japan, ³Wallenberg Neuroscience Center, Lund University, SE-221 84 Lund, Sweden, ⁴Department of Neurology, Jichi Medical University, Tochigi 329-0498, Japan, ⁵Department of Pharmacology, Fujita Health University School of Medicine, Toyoake, Aichi 470-1192, Japan, ⁶Department of Functional Genomics Institut de Génétique et Biologie Moléculaire et Cellulaire, 67404 Illkirch, France, Departments of ⁷Neuroscience, ⁸Laboratory Medicine, and ⁹Cell and Molecular Biology, Karolinska Institutet, SE-171 77 Stockholm, Sweden, and ¹⁰Max Planck Institute for Biology of Ageing, D-50931 Cologne, Germany

Transcription factors involved in the specification and differentiation of neurons often continue to be expressed in the adult brain, but remarkably little is known about their late functions. *Nurr1*, one such transcription factor, is essential for early differentiation of midbrain dopamine (mDA) neurons but continues to be expressed into adulthood. In Parkinson's disease, *Nurr1* expression is diminished and mutations in the *Nurr1* gene have been identified in rare cases of disease; however, the significance of these observations remains unclear. Here, a mouse strain for conditional targeting of the *Nurr1* gene was generated, and *Nurr1* was ablated either at late stages of mDA neuron development by crossing with mice carrying Cre under control of the dopamine transporter locus or in the adult brain by transduction of adeno-associated virus Cre-encoding vectors. *Nurr1* deficiency in maturing mDA neurons resulted in rapid loss of striatal DA, loss of mDA neuron markers, and neuron degeneration. In contrast, a more slowly progressing loss of striatal DA and mDA neuron markers was observed after ablation in the adult brain. As in Parkinson's disease, neurons of the substantia nigra compacta were more vulnerable than cells in the ventral tegmental area when *Nurr1* was ablated at late embryogenesis. The results show that developmental pathways play key roles for the maintenance of terminally differentiated neurons and suggest that disrupted function of *Nurr1* and other developmental transcription factors may contribute to neurodegenerative disease.

Introduction

Adaptation to a changing environment requires plasticity in the adult CNS. However, to ensure that neurons are properly maintained, such plasticity must be balanced against mechanisms that counteract phenotypic instability. Studies of how neurons develop may help to unravel functions important for the stability of nerve cells as factors promoting their differentiation may also contribute to their maintenance. Indeed, many transcription fac-

tors identified for their critical roles during neuronal development continue to be expressed in the postnatal nervous system, raising the possibility that they contribute to the integrity of already differentiated neurons (Hendricks et al., 1999; Vult von Steyern et al., 1999; Kang et al., 2007; Alavian et al., 2008). However, the consequences of adult gene ablation of any of these factors have not yet been reported, and very little is known of their functions in differentiated neurons.

From a clinical perspective, it is of particular interest to identify factors that maintain stability of neurons that are affected in neurodegenerative disorders as loss of phenotype would likely cause or contribute to disease. Parkinson's disease (PD) is characterized by progressive pathology of midbrain dopamine (mDA) neurons of substantia nigra pars compacta (SNc) and the ventral tegmental area (VTA), typically involving deposition of α -synuclein-rich cytoplasmic protein aggregates termed Lewy bodies. During development, early signaling events induce transcription factors that control the specification and differentiation of mDA neurons (Smidt and Burbach, 2007). Several of these factors, including *Nurr1*, *Lmx1a*, *Lmx1b*, *Pitx3*, *FoxA2*, and *En1/2*, continue to be expressed in the postnatal and adult brain (Zetterström et al., 1996; Smidt et al., 1997, 2000; Albéri et al., 2004; Simon et al., 2004; Kittappa et al., 2007). *Nurr1*, belonging to a family of ligand-independent nuclear receptors (Wang et al.,

Received Aug. 11, 2009; revised Oct. 17, 2009; accepted Oct. 28, 2009.

This work was supported by grants from the Michael J. Fox Foundation (T.P., A.B., L.O.), Vetenskapsrådet via Linné Center DBRM (T.P.), Grants-in-Aid for Human Frontier Science Program (P.C., D.M., H.I.), Grants-in-Aid for Scientific Research from the Ministry of Education, Culture, Sports, Science, and Technology of Japan, the Ministry of Health, Labor, and Welfare of Japan, and the Japan Science and Technology Agency, Core Research for Evolutional Science and Technology (S.-I.M., H.I.), Vetenskapsrådet (L.O.), Swedish Brain Power (L.O.), Swedish Brain Foundation (L.O.), and the Swedish Parkinson Foundation (L.O.). We are grateful to Johan Ericson and members of the Perlmann and Ericson laboratories for valuable discussions. We thank Andrée Dierich and Jean-Marc Bornert for their help in mouse mutagenesis, Noriko Ihira for help in construction of the targeting vector and screening of ES clones, Björn Arnelius and Naomi Takino for their help with AAV vectors, Ulla Jarl for help with histology, and Marie-Louise Alun for advice on mice handling.

Correspondence should be addressed to either of the following: Thomas Perlmann, Department of Cell and Molecular Biology, Karolinska Institutet, SE-171 77 Stockholm, Sweden, E-mail: thomas.perlmann@licr.ki.se; or Hiroshi Ichinose, Graduate School of Bioscience and Biotechnology, Tokyo Institute of Technology, Yokohama 226-8501, Japan, E-mail: hichinos@bio.titech.ac.jp.

DOI:10.1523/JNEUROSCI.3910-09.2009

Copyright © 2009 Society for Neuroscience 0270-6474/09/2915923-10\$15.00/0

2003; Perlmann and Wallén-Mackenzie, 2004), becomes expressed in developing mDA neurons that have just exited the cell cycle and is essential for mDA neuron development because mDA neurons of both the SNc and VTA fail to express dopaminergic markers and newborn *Nurr1*-null mice lack mDA neuron cell bodies and their striatal projections (Zetterström et al., 1997; Castillo et al., 1998; Saucedo-Cardenas et al., 1998). How *Nurr1* regulates target genes in mDA neuron development remains essentially unknown but may involve a functional interaction with the homeobox transcription factor *Pitx3* (Jacobs et al., 2009).

Determining the role of *Nurr1* also in the adult brain is of particular importance because previous studies suggested an association of this protein with PD pathology. *Nurr1* expression is diminished in neurons with α -synuclein inclusions in postmortem PD brain tissue, and *Nurr1* mutations and polymorphisms have been identified in rare cases of PD (Xu et al., 2002; Le et al., 2003; Zheng et al., 2003; Grimes et al., 2006). However, the significance of genetic lesions remain unclear (Wellenbrock et al., 2003; Hering et al., 2004; Tan et al., 2004). These observations emphasize the importance of elucidating the role of *Nurr1* in more mature mDA neurons by analyzing the consequences of conditional *Nurr1* gene ablation in mice.

Materials and Methods

Conditional *Nurr1* gene-targeted mice. Mouse 129SV genomic library constructed in bacterial artificial chromosome (BAC) was screened by PCR. A BAC clone containing the entire *Nurr1* gene was selected, and a BamHI–MunI fragment containing exon 1 to exon 5 was recloned into a pBluescript II vector. A floxed neomycin cassette was inserted into an internal EcoRI site located in intron 3, and a synthetic loxP sequence was inserted at SalI site located in intron 2. Mouse embryonic stem (ES) cells were electroporated with the targeting vector, and the homologously recombined clones were screened by PCR and Southern blot analysis. ES clones with three loxP sites were selected, and a plasmid expressing Cre DNA recombinase was transiently transfected into the cells. ES cells with two loxP sites without a neomycin cassette were selected by PCR and used for production of chimeric mice.

Animals. Mice were kept in rooms with controlled 12 h light/dark cycles, temperature, and humidity, with food and water provided *ad libitum*. All animal experiments were performed with permission from the local animal ethics committee. The generation of dopamine transporter (*DAT*)–*Cre* mutant mice has been described previously (Ekstrand et al., 2007). Mice were mated during the night, and the females were checked for vaginal plugs in the morning [day of vaginal plug considered as embryonic day 0.5 (E0.5)].

L-3,4-Dihydroxyphenylalanine treatment. Methyl L-3,4-dihydroxyphenylalanine (L-DOPA) hydrochloride and the peripheral DOPA decarboxylase inhibitor benserazide-HCl (Sigma-Aldrich) were dissolved in Ringer's solution immediately before use. L-DOPA was intraperitoneally given every second day at the dose of 2.5 mg/kg combined with 0.625 mg/kg benserazide. Chronic treatment with L-DOPA/benserazide was administered for 50 d, starting at postnatal day 15 (P15). During this period, the mice were carefully observed and weight was measured regularly. Reported hyperactivity was observed in *cNurr1^{DATCre}* mice when given a single higher dose of L-DOPA (25 mg/kg L-DOPA, 6.25 mg/kg benserazide).

Histological analyses. At embryo stages, embryos were fixed for 2–24 h in 4% phosphate-buffered paraformaldehyde (PFA), cryopreserved in 30% sucrose before being embedded in OCI (Sakura Finetek), and cryosectioned at a thickness of 10–20 μ m onto slides (SuperFrostPlus; Menzel Gläser). For the isolation of brains for immunolabeling at P15 and onward, animals were anesthetized with Avertin (tribromoethanol; 0.5 mg/g) and perfused through the left ventricle with body-temperature PBS, followed by ice-cold 4% PFA. The brains were dissected and post-fixed overnight in 4% paraformaldehyde and subsequently cryoprotected for 24–48 h in 30% sucrose at 4°C. The brains were serially sectioned on a cryostat or sliding microtome at 10–30 μ m. Littermates were used in an all comparative experiments.

For immunohistochemistry, sections were preincubated for 1 h in blocking solution containing either 10% normal goat sera or 5–10% bovine serum albumin, 0.25% Triton X-100, and 0.01% Na-azide in PBS. Primary antibodies diluted in blocking solution were applied overnight at 4°C. After rinses with PBS, biotinylated- or fluorophore-conjugated secondary antibodies diluted in PBS were applied for 1 h at room temperature. Biotinylated secondary antibodies were followed by incubation with streptavidin–horseradish peroxidase complex (ABC elite kit, Vectastain) for 1 h and subsequent exposure to diaminobenzidine (DAB kit; Vector Laboratories). Primary antibodies and dilution factors were as follows: rabbit anti-*Nurr1* (1:100; M196; Santa Cruz Biotechnology), anti-*Nurr1* (1:250; E20; Santa Cruz Biotechnology), rabbit anti-tyrosine hydroxylase (TH) (1:500; Pel-Freez), rat anti-DAT (1:2000; Millipore Bioscience Research Reagents), mouse anti-TH (1:200; Millipore Bioscience Research Reagents), rabbit anti-vesicular monoamine transporter (VMAT) (1:500; Millipore Bioscience Research Reagents), rabbit anti-L-DOPA decarboxylase (AADC) (1:500; Millipore Bioscience Research Reagents), rabbit anti-*Cre* (1:10,000; Covance Research Products), guinea pig anti-*Lmx1b* (1:1000) (Andersson et al., 2006), and rabbit anti-*Pitx3* (Smidt et al., 2004). In some cases (anti-AADC, anti-VMAT, and anti-*Nurr1*), the blocking steps were performed after antigen retrieval (Dako). Finally, expression was detected by secondary antibodies from Jackson ImmunoResearch. Section images were collected by confocal microscopy (Leica DMIRE2) and bright-field microscopy (Eclipse E1000K; Nikon). Cell counting was performed by counting all SNc DA neurons detected by immunohistochemistry (DAB) in a total of three sections per animal (every 12th tissue section) within the ventral midbrain of animals taken at 4 months after vector injection in both wild-type *wt^A-AVCre* and *cNurr1^{AAVCre}* animals. The mean of counted cells per animal was established from both the injected and non-injected sides in each animal, and the relative decrease was calculated as a percentage as described in Results.

AAV-*Cre* injections. Two and a half- to 5-month-old animals received one unilateral stereotaxic injection in the right striatum using a 10 μ l Hamilton microsyringe fitted with a glass pipette tip. The animals were anesthetized with isoflurane, 1 μ l was injected during 5 min, and the cannula was left in place for an additional 2 min before being slowly retracted. The anteroposterior and mediolateral coordinates from bregma were -2.8 and -1.1 mm, respectively, and the dorsoventral coordinates from the dura were -4.3 mm. Animals were killed 0.5, 1.5, and 4 months after injection, and the brains were isolated.

Measurement of tissue content for dopamine, serotonin, and their metabolites. In supplemental Tables 1–3 (available at www.jneurosci.org as supplemental material), tissues were collected from P1, P7, P14, and adult (P48) *wt^{DATCre}* and *cNurr1^{DATCre}* mice. One- to 14-d-old mice were killed by decapitation, and P48 mice were killed by cervical dislocation. Brains were rapidly removed, chilled in saline (4°C), dissected, frozen on dry ice, and stored at -80°C until use. To process tissues for HPLC and electrochemical detection of monoamines and metabolites, samples were homogenized by sonication in 5 vol or in 30 μ l of 0.1 M perchloric acid, followed by centrifugation. Endogenous levels of noradrenaline, DA, 3,4-dihydroxyphenylacetic acid, homovanillic acid (HVA), serotonin (5-HT), and 5-hydroxyindoleacetic acid were determined in the supernatants. A reverse column (BAS, C-18, 100.0 \times 3.2 mm, 3 μ m particle diameter) was used for separation. The mobile phase consisted of 0.05 M sodium phosphate/0.03 M citric acid buffer containing 0.1 mM EDTA and was adjusted with various amounts of methanol and sodium-L-octane sulfonic acid. The flow rate was 0.3 ml/min. Monoamines and metabolites were detected using a glassy-carbon electrode detector, which as set at +0.7 V versus an Ag/AgCl reference electrode. Resultant peaks were measured and compared with repeated control samples containing fixed mixed amounts of compounds of interest.

In supplemental Table 4 (available at www.jneurosci.org as supplemental material), all animals were killed, and striata and cortex were rapidly dissected out, frozen on dry ice, and stored at -80°C . To determine monoamines, tissue was homogenized in 0.1 M perchloric acid and centrifuged at 10,000 rpm for 10 min before filtering through minispin filters for an additional 3 min at 10,000 rpm. The tissue extract were then analyzed by HPLC as described previously (Carta et al., 2007) with minor

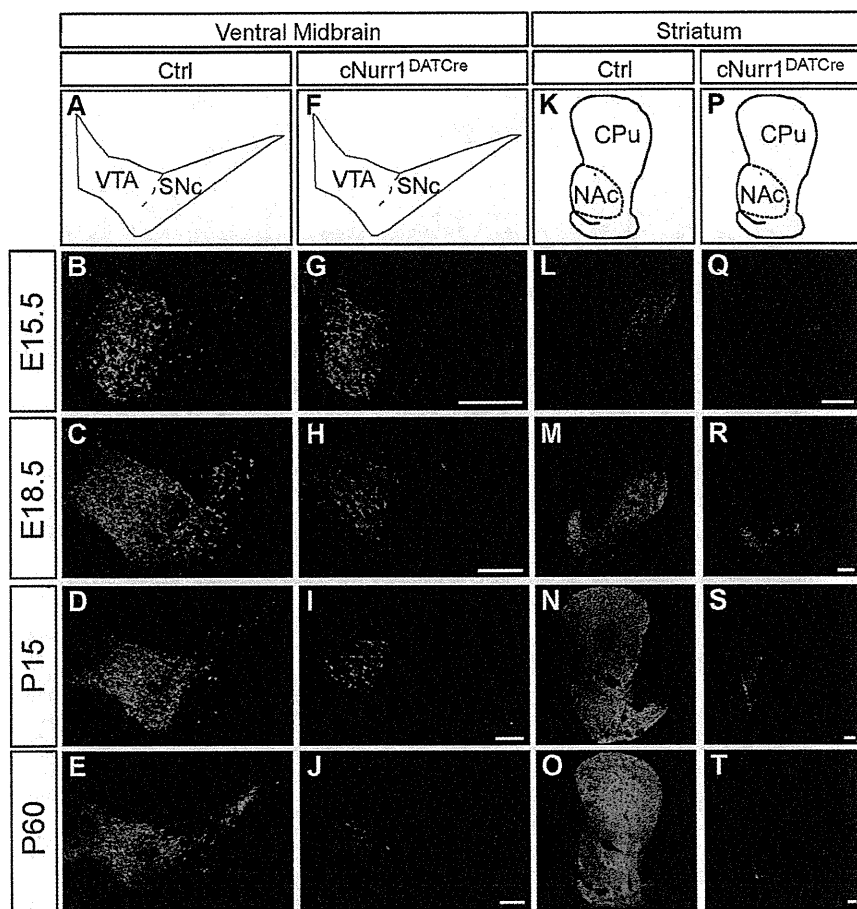


Figure 1. TH is progressively lost in both the ventral midbrain and striatum of *cNurr1^{DATCre}* mice. **A–T**, Confocal microscopy showing TH immunohistochemistry in control (ctrl) and *cNurr1^{DATCre}* mice as indicated. **A–J**, Sections were analyzed at the levels of ventral midbrain (as indicated in **A** and **F**) and in the striatum (as indicated in **K** and **P**). TH immunofluorescence was analyzed at both embryonal and postnatal stages as indicated. Results demonstrate a progressive loss of TH immunoreactivity in the ventral midbrain. Note that TH immunoreactivity was more drastically downregulated at more lateral regions compared with the prospective medial VTA. **K–T**, TH immunoreactivity in the striatum. In *cNurr1^{DATCre}* mice, TH was lost in the CPU and diminished in the NAc. Scale bars, 250 μ m.

modifications. Briefly, 25 μ l of each sample were injected by a cooled autosampler (Midas) into an ESA Coulochem III coupled with an electrochemical detector. The mobile phase (5 g/L sodium acetate, 30 mg/L Na₂-EDTA, 100 mg/L octane-sulfonic acid, and 10% methanol, pH 4.2) was delivered at a flow rate of 500 μ l/min to a reverse-phase C18 column (4.6 mm diameter, 150 mm).

Fluorogold retrograde tracing. Animals received one unilateral stereotaxic injection in the right striatum using a 5 μ l Hamilton microsyringe (22 gauge steel cannula) filled with the retrograde tracer Fluorogold (hydroxystilbamidine, 4%, Biotium). The animals were anesthetized with isoflurane, 0.5 μ l was injected during 1 min, and the cannula was left in place for an additional 2 min before slowly being retracted. The anteroposterior and mediolateral coordinates from bregma were 0.27 and –2.10 mm, respectively, and the dorsoventral coordinates from the dura were –2.60 mm. Animals were killed 4 d after injection, and the brains were isolated. Fresh-frozen sections (14 μ m) were cut with a cryostat and examined under a epifluorescence microscope (Eclipse E1000K; Nikon) coupled to an RTke spot camera.

Open-field test. This test was used to monitor overall activity and rearing behavior. The open field consisted of a white plastic box (55 \times 35 \times 30 cm) with lines (squares of 7 \times 35 cm) painted on its floor. The animals were put in the center of the box, habituated for 10 min, and filmed 15 min thereafter while rearing was scored. The video recordings were used to measure the number of lines crossed during the monitoring period. A

line crossing was counted when the mouse moved its whole body from one square to another.

Stepping test. Forelimb akinesia was monitored in a modified version of the stepping test, as described previously for rats (Schallert et al., 1992; Kirik et al., 1998). The test was performed three times daily over 3 consecutive days. In this test, the mouse was held firmly by the experimenter with both hindlimbs and one forelimb immobilized, and the mouse was passively moved with the free limb contacting a table surface. The number of adjusting steps, performed by the free forelimb when moved in the forehand and backhand directions, over a distance of 30 cm, was recorded. Results are presented as data collected on the third testing day.

Results

Selective *Nurr1* ablation in late developing mDA neurons

A mouse strain containing a *Nurr1* allele for conditional gene ablation was generated by insertion of two loxP sequences in the second and third introns so that the coding sequence, including the first coding exon 3, is excised by Cre-mediated recombination (supplemental Fig. 1, available at www.jneurosci.org as supplemental material). To analyze the consequences of *Nurr1* ablation at late stages of mDA neuron development, we crossed floxed *Nurr1* mice with mice carrying *Cre* inserted in the locus of the *DAT* gene (Ekstrand et al., 2007). Crosses generated *Nurr1* mice that were homozygous for the conditional targeted *Nurr1* allele and heterozygous for the *DAT–Cre* allele (*Nurr1^{L2/L2};DAT^{Cre/wt}*; hereafter referred to as *cNurr1^{DATCre}* mice). Littermates of genotype *Nurr1^{L2/L2};DAT^{wt/wt}* or *Nurr1^{wt/wt};DAT^{Cre/wt}* were used as controls. Although we cannot ex-

clude that a small number of cells escape *Nurr1* gene deletion, immunohistochemistry using an antibody against *Nurr1* showed that *DAT–Cre*-mediated *Nurr1* ablation resulted in the expected delayed loss of *Nurr1* expression in mDA neurons beginning from approximately E13.5 and becomes essentially complete at E15.5 (supplemental Fig. 2, available at www.jneurosci.org as supplemental material). At this stage of normal development, cells express pan-neuronal properties as well as many mDA neuron markers, and axons are growing toward the developing striatum (Smidt and Burbach, 2007).

cNurr1^{DATCre} mice were born at the expected Mendelian frequency of ~25% (of a total $n = 159$); however, *cNurr1^{DATCre}* mice were less active than controls and did not survive beyond 3 weeks after birth. If litters were allowed to remain with their mothers after weaning, perinatal death was avoided in ~50% of *cNurr1^{DATCre}* pups. These surviving mice were, however, ~40% smaller than controls at the age of 2 months (supplemental Fig. 3, available at www.jneurosci.org as supplemental material). Although no significant change in spontaneous light-phase locomotor activity could be observed in adult *cNurr1^{DATCre}* mice, rearing was dramatically decreased (supplemental Fig. 3, avail-

able at www.jneurosci.org as supplemental material). L-DOPA treatment of mutant mice did not improve viability and did not induce any weight gain. Instead, *cNurr1^{DATCre}* mice display a pronounced and severe hypersensitivity to L-DOPA treatment characterized by an acute phase of hyperactivity and repetitive behaviors (including repetitive gnawing, excessive grooming, and self-injury) in all tested mutant ($n = 9$) but not in any wild-type controls ($n = 7$) (see Materials and Methods). These behaviors resemble those that have been observed in neonatal 6-hydroxydopamine lesioned rats treated with L-DOPA (Breese et al., 2005). In conclusion, late embryonic mDA neuron-selective *Nurr1* ablation is associated with decreased weight, rearing, and viability, and mice show an altered response to L-DOPA.

Reduced levels of TH and DA in brains of *cNurr1^{DATCre}* mice

The observed abnormalities are consistent with a dopaminergic deficiency. To analyze the possible cellular basis for the phenotype, brain sections from controls and *cNurr1^{DATCre}* mice were analyzed by immunohistochemistry using an antibody against TH (Fig. 1). A progressive loss of TH immunostaining in SNc was observed in the *cNurr1^{DATCre}* mice (Fig. 1*A–J*). TH levels were significantly decreased already at E15.5, soon after *Nurr1* is lost, and decreased further until adulthood when only scattered TH-positive neurons could be detected. TH was diminished also within the VTA at later stages, but a significant number of cells remained even in adult animals (Fig. 1*A–J*). These cells were counted in four non-consecutive sections for each analyzed brain. In adult control VTA, a mean of 74.5 ± 7.1 cells per section were counted in *cNurr1^{DATCre}* mice ($n = 4$) and 499.3 ± 5.2 cells in controls ($n = 3$) (Student's *t* test, 4.4×10^{-7}). TH immunostaining within the caudatus putamen (CPu) was completely lost (Fig. 1*K–T*). However, weak immunoreactivity remained in nucleus accumbens (NAc) innervated preferentially by VTA neurons (Fig. 1*K–T*). We also noted the appearance of ectopic TH-positive cell bodies within the striatal parenchyma in *cNurr1^{DATCre}* mice (supplemental Fig. 4, available at www.jneurosci.org as supplemental material). These cells were more frequent in regions in which striatal TH had been most severely depleted as a consequence of *Nurr1* ablation and resemble TH-positive neurons appearing in rodent and primate DA-depletion models (Huot and Parent, 2007). Decreased levels of TH immunostaining were paralleled by decreased DA levels, as measured by HPLC (supplemental Tables 1–3, available at www.jneurosci.org as supplemental material). Striatal DA was dramatically reduced to 14% of controls at P1 in *cNurr1^{DATCre}* mice and was almost completely lost by P60. An increased ratio of HVA to DA at P14 indicated increased turnover of DA in remaining cells at this stage (supplemental Table 2, available at www.jneurosci.org as supplemental mate-

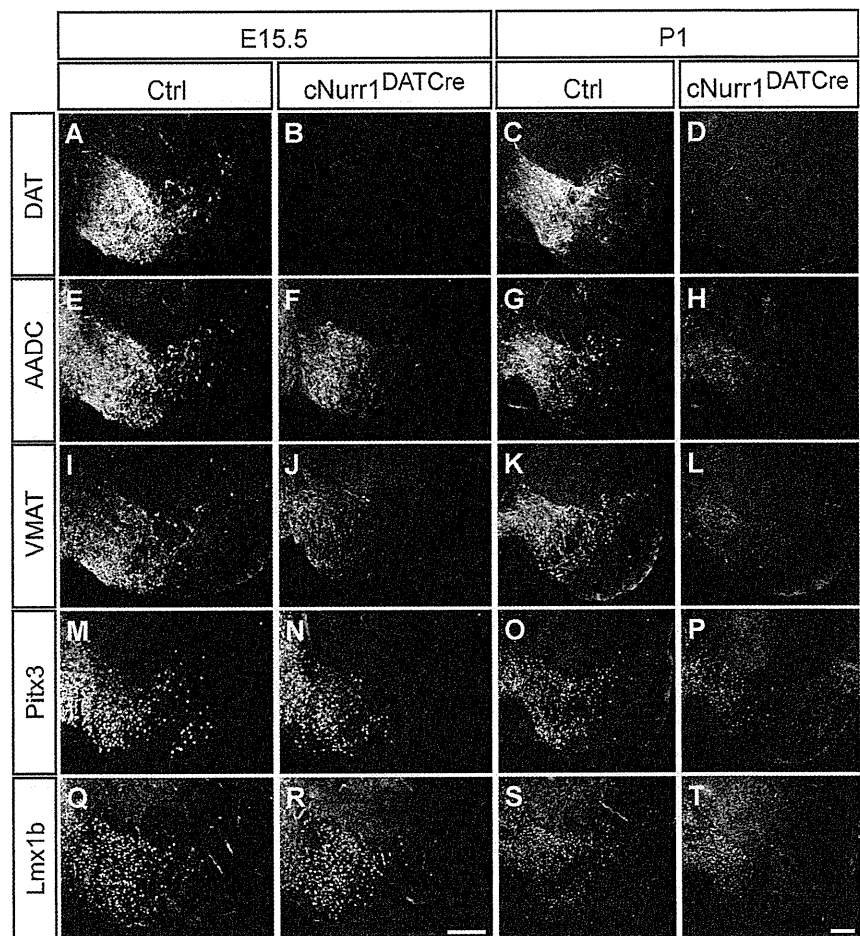


Figure 2. All analyzed mDA neuron markers are lost or diminished in *cNurr1^{DATCre}* mice. *A–T*, Confocal microscopy showing immunohistochemistry of several different mDA neuron markers in control (ctrl) and in *cNurr1^{DATCre}* mice at E15.5 or at P1, as indicated. The following markers were analyzed: DAT, AADC, VMAT, Pitx3, and Lmx1b. Results show a progressive loss of markers that is more substantial in the lateral SNc, whereas more medial VTA cells are lost more slowly. DAT is completely absent already at E15.5 in *cNurr1^{DATCre}* mice, whereas all other markers are decreased more slowly in this area (compare *A, B*). Scale bars, 200 μ m.

rial). DA was more severely decreased in CPu compared with NAc (supplemental Table 3, available at www.jneurosci.org as supplemental material). In contrast, 5-HT was significantly increased in both CPu and NAc, consistent with previous findings showing increased serotonergic innervation after striatal DA depletion (Snyder et al., 1986). Thus, a severe neurotransmitter deficiency of the mesostriatal DA system is apparent in *cNurr1^{DATCre}* mice. Together, measurements of TH immunoreactivity and DA levels demonstrate that *Nurr1* is critically required for maintaining TH expression and DA synthesis from late stages of mDA neuron differentiation.

Cellular deficiency within the ventral midbrain of *cNurr1^{DATCre}* mice

To investigate whether the phenotype is a consequence of a more limited disruption of DA synthesis or a more severe cellular deficiency, a number of additional mDA neuron markers were analyzed. All analyzed mDA neuron markers were diminished or absent within SNc in *cNurr1^{DATCre}* mice already at E15.5 (Fig. 2). DAT was completely lost at E15.5 and therefore, consistent with previous data (Sacchetti et al., 1999), stands out as being a likely direct target of *Nurr1* (Fig. 2*A–D*). Additional control experiments showed that DAT and other markers, including TH and

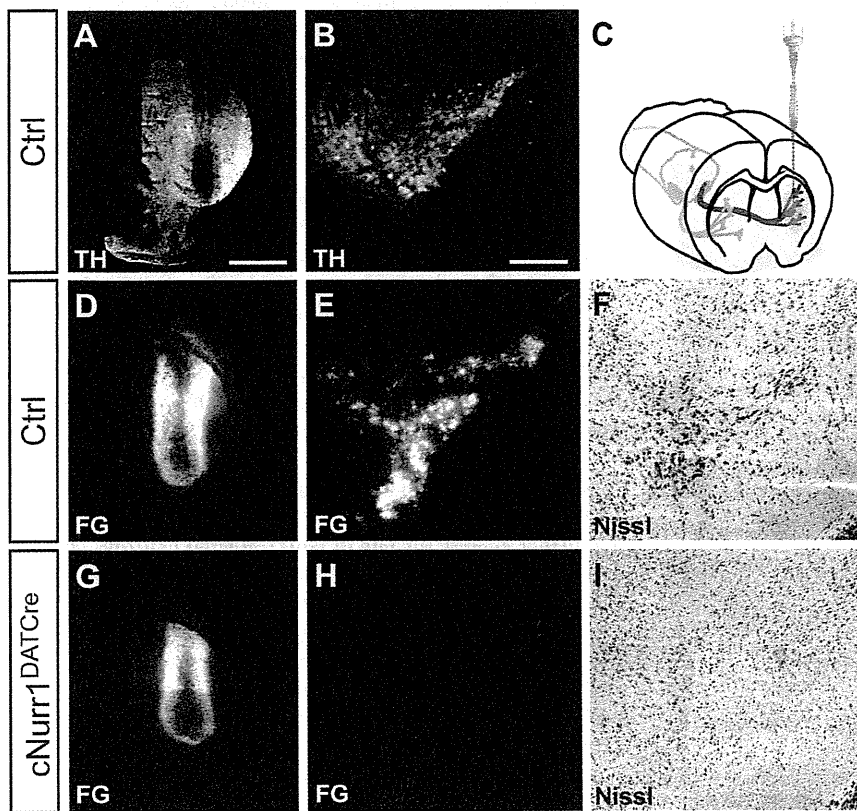


Figure 3. Cell bodies and striatal innervation are lost in *cNurr1*^{DATCre} mice as determined by Fluorogold (FG) retrograde tracing of fibers extending from cell bodies in SNc to the striatum. **A–C**, After Fluorogold injection, injected into the left striatum in either adult (1.5 months old) control (Ctrl) or *cNurr1*^{DATCre} mice as indicated in **C**, mice were killed after 4 d and analyzed for TH immunofluorescence in the striatum (**A**) or ventral midbrain (**B**). **D–I**, Analysis for Fluorogold (FG) or by Nissl staining. Strong Fluorogold staining in both striatum (**D**) and in the ventral midbrain (**E**) was consistently seen in all control (Ctrl) animals ($n = 7$). In contrast, Fluorogold fluorescence was only detected in the striatum (**G**) in *cNurr1*^{DATCre} mice ($n = 5$), indicating that fibers from the SNc (**H**) had been lost in these animals. Moreover, large, densely packed cell bodies are only visualized by Nissl staining in the ventral midbrain of control animals (**F**) but are completely absent from *cNurr1*^{DATCre} mice (**I**). Striatal site of Fluorogold injection is marked by asterisk in **A**, **D**, and **G**. Scale bars: **A**, **B**, **D**, **E**, **G**, **H**, 1 μm ; **F**, **I**, 1200 μm .

Nurr1, were not visibly decreased in mice heterozygous for the *DAT-Cre* allele (supplemental Fig. 5, available at www.jneurosci.org as supplemental material) (data not shown). In contrast to DAT, AADC, VMAT2, Pitx3, or Lmx1b were not reduced within the most medial ventral midbrain at this early stage and, with the exception of DAT, markers were not completely downregulated at P1 (Fig. 2E–T). The progressive loss of markers indicates a severe loss of phenotype within the SNc, whereas cells within the VTA appear more resilient. Importantly, most TH-positive cells within the VTA have lost any detectable expression of DAT, indicating that these cells have not escaped Nurr1 gene targeting (supplemental Fig. 6, available at www.jneurosci.org as supplemental material).

To further assess the extent of a cellular deficiency, striatal target innervation was analyzed by Fluorogold retrograde tracing after injection into the striatum of live 8- to 9-week-old controls and *cNurr1*^{DATCre} mice. Fluorogold was transported into SNc cell bodies of control mice; however, fluorescence was entirely undetected within the SNc of Fluorogold-injected *cNurr1*^{DATCre} mice (Fig. 3, compare **D**, **E** with **G**, **H**). In addition, characteristic large and densely packed TH-immunoreactive mDA neurons within the SNc were virtually absent in *cNurr1*^{DATCre} mice (Fig. 3I). In conclusion, Nurr1 ablation in *cNurr1*^{DATCre} mice results in rapid loss of SNc cell bodies; however, scattered VTA neurons remained even in adult *cNurr1*^{DATCre} mice.

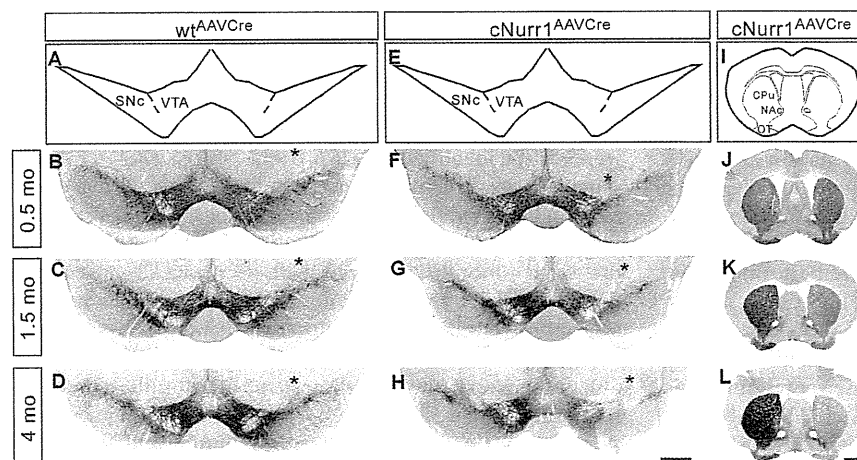


Figure 4. TH expression in both the ventral midbrain and striatum is progressively lost in the injected, but not non-injected, side of *cNurr1*^{AAVCre} mice. **A–H**, Sections from 0.5, 1.5, and 4 month (mo; as indicated) old AAV–Cre-injected controls (*wtAAVCre*) or *cNurr1*^{AAVCre} mice were used for analyses by nonfluorescent DAB TH immunostaining in the ventral midbrain. The analyzed region within the ventral midbrain is schematically illustrated in **A** and **E**. The site of injection, marked by an asterisk in **B–D** and **F–H**, was verified in all animals by high-power magnification microscopy and was identified as a small area of injection-induced necrosis. Results show that TH immunostaining is not drastically altered at 0.5 months but is progressively decreased at 1.5 and 4 months in the injected SNc and VTA. **I–L**, DAB TH staining at the level of striatum. Analyzed regions are indicated in **I**. TH staining is progressively decreased at 1.5 and 4 months in the side that is ipsilateral to the side of AAV–Cre injection in *cNurr1*^{AAVCre} mice (**J–L**). OT, Olfactory tubercle. Scale bars: **A–H**, 600 μm ; **I–L**, 1 mm.

Adeno-associated virus–Cre-mediated *Nurr1* ablation in adult mice

In *cNurr1*^{DATCre} mice, *Nurr1* is ablated well before full mDA neuron maturity and before targets in the striatum have become innervated; thus, it remained possible that the phenotype is a consequence of a developmental dysfunction. Therefore, we proceeded to inactivate *Nurr1* specifically in ventral midbrain of adult mice, using an adeno-associated virus (AAV)–Cre vector driven by the neuron-specific synapsin promoter. AAV–Cre was administered by unilateral stereotaxic microinjection above the right SNc. Cre immunohistochemistry and β -galactosidase expression was analyzed after intranigral AAV–Cre injection into reporter mice in which the ROSA26 locus is targeted with a LacZ reporter gene (Soriano, 1999). Results show widespread Cre expression around the site of injection, spreading into both SNc and VTA, and robust recombination of the LacZ reporter construct (supplemental Fig. 7, available at www.jneurosci.org as supple-

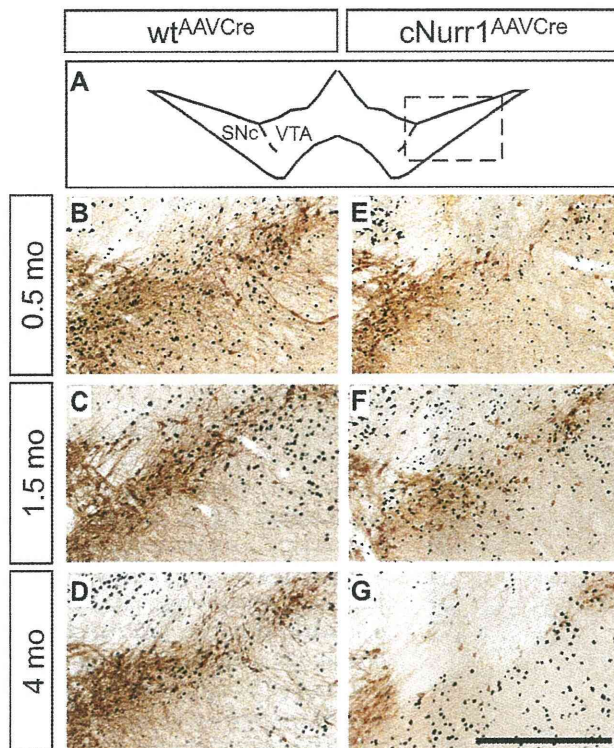


Figure 5. Cre-expressing cells are lost at 4 months within the SNc after Nurr1 ablation. **A**, Higher magnification showing TH by DAB staining (brown) at the level of the injected SNc in *wtAAVCre* and *cNurr1AAVCre* mice. The region that has been magnified is boxed in **A**. **B–G**, Adjacent sections were immunostained for Cre (black) and are superimposed on the DAB-stained TH sections in all micrographs. Cre staining is widespread in the area in which mDA neurons are normally localized at 0.5 and 1.5 months (**E**, **F**) but almost completely absent in this area at 4 months (**G**). Scale bar, 500 μ m.

mental material). Moreover, except for a small necrotic area around the site of injection, virus administration did not affect tissue morphology, expression of mDA neuron markers, or microglia activation (data not shown).

AAV-Cre was unilaterally injected above the SNc of adult mice homozygous for the floxed *Nurr1* allele to generate adult conditional gene-targeted mice (*cNurr1AAVCre*) or into wild-type control mice (*wtAAVCre*). In addition, a vector encoding the green fluorescent protein (GFP) driven by the synapsin promoter (AAV-GFP) was injected in mice homozygous for the floxed *Nurr1* allele (*cNurr1AAV-GFP* mice) to ensure that the floxed animals are not more sensitive to nonspecific toxicity induced by AAV transduction. Histological analyses were performed from animals killed at 0.5, 1.5, and 4 months after injection.

Reduction of TH and DA in adult *Nurr1*-ablated mice

TH immunohistochemistry at the level of the ventral midbrain was analyzed to assess the consequences of adult *Nurr1* ablation. Within SNc, TH immunoreactivity was unaffected at 0.5 months but was progressively reduced at 1.5 and 4 months in the injected SNc in *cNurr1AAVCre* mice (Fig. 4E–H). In contrast, TH immunoreactivity was unaffected in SNc of control *wtAAVCre* and *cNurr1AAV-GFP* mice (Fig. 4A–D) (data not shown). TH was also reduced in the VTA at 1.5 and 4 months; however, at 4 months, the reduction in VTA was less dramatic compared with SNc (Fig. 4E–H).

Decreased striatal TH immunoreactivity paralleled the reduction in the ventral midbrain. Thus, although no signs of degen-

erating striatal TH-stained fibers (swollen axons or dystrophic neurites) were detected, striatal sections ipsilateral to the side of AAV-Cre injection showed clearly reduced TH in *cNurr1AAVCre* mice but not in controls (*wtAAVCre* or *cNurr1AAV-GFP*) (Fig. 4I–L) (supplemental Fig. 8, available at www.jneurosci.org as supplemental material). Diminished TH immunoreactivity was observed in regions innervated by both SNc and VTA (CPU and NAc, respectively), consistent with the reduced TH immunoreactivity in both SNc and VTA mDA neuron cell bodies. Measurement of DA and metabolites by HPLC from dissected tissue at 4 months confirmed this picture as a significant reduction in DA and DA metabolites noted both within the dorsolateral striatum and in areas mostly innervated by the VTA (cortex and ventromedial striatum) (supplemental Table 4, available at www.jneurosci.org as supplemental material). Thus, TH, DA, and DA metabolites are clearly reduced as a result of adult *Nurr1* ablation.

Loss of mDA neuron characteristics in adult *Nurr1*-ablated mice

To further analyze the fate of *Nurr1*-ablated neurons, cells were counted within the SNc and VTA in *cNurr1AAVCre* and *wtAAVCre* mice. Within SNc, the number of TH-positive cells was significantly decreased at 4 months (58.1 ± 8.3 and $95.4 \pm 6.3\%$ in the injected vs non-injected sides of *cNurr1AAVCre* and *wtAAVCre* mice, respectively; $p = 0.0053$). In contrast, the numbers of TH-positive cells was not significantly reduced within the VTA (104.1 ± 4.7 and $101.6 \pm 10.5\%$ in the injected versus non-injected sides of *cNurr1AAVCre* and *wtAAVCre* mice, respectively). Also, the numbers of TH-positive cells were not significantly changed in *cNurr1AAVCre* mice at 1.5 months (data not shown).

To assess the integrity of neurons, cellular analysis was extended by analyzing Cre-immunolabeled sections that were superimposed on adjacent TH-labeled sections (Fig. 5). Notably, in *cNurr1AAVCre* mice, Cre expression was clearly detected within the area of SNc at both 0.5 and 1.5 months but was lost at 4 months in the region in which mDA neurons should normally be localized (Fig. 5, compare E–G with B–D). Cre expression is driven by a general neuronal promoter (synapsin), suggesting that loss of *Nurr1* may eventually affect some pan-neuronal properties at 4 months after ablation.

Confocal microscopy confirmed the loss of TH at 1.5 and 4 months after *Nurr1* ablation and the loss of Cre at 4 months (Fig. 6A–D). At 1.5 months, DAT expression was weak but cell bodies were readily identified (Fig. 6E, F and inset in F). DAT staining remained also at 4 months, but, at this stage, high-power magnification indicated that some of the staining appeared confined to fibers and/or dystrophic cells (Fig. 6G, H and inset in H). Nonetheless, at 4 months, most cells with decreased TH stained positive for AADC, showing that not all mDA neuron characteristics were affected (Fig. 7A–F). Moreover, VMAT2 is yet another marker that was severely decreased in *cNurr1AAVCre* mice, but remaining weakly stained cells were positive for the general neuronal marker Hu (Fig. 7G–L). The observed changes were not correlated to increased number of apoptotic cells because increased activated Caspase 3 could not be detected (data not shown). Also, we found no evidence for nigral inflammation or α -synucleinopathy because activated microglia and α -synuclein-rich inclusions were not detected at any stage after *Nurr1* ablation in *cNurr1DATCre* mice (data not shown). Finally, TH and DAT expression in VTA was also affected, without any apparent loss of the neuronal marker Hu or any signs of dystrophic cells (supplemental Fig. 9, available at www.jneurosci.org as supplemental material) (data not shown). Thus, *Nurr1* ablation results in a

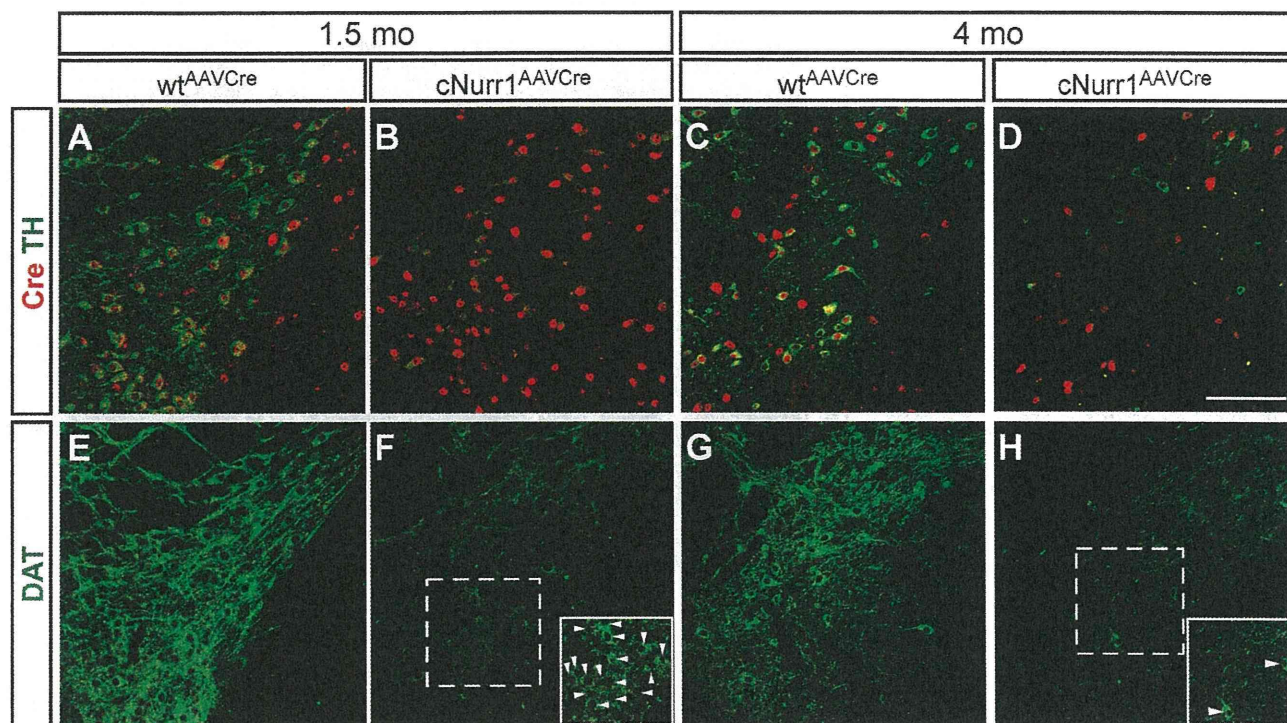


Figure 6. Decreased expression of DAT and signs of dystrophic cells in *cNurr1^{AAVCre}* mice. **A–H**, Confocal analysis of SNc in *wt^{AAVCre}* and *cNurr1^{AAVCre}* mice at 1.5 and 4 months, as indicated. Confocal images show double staining of Cre (red) and TH (green; **A–D**) and staining for DAT (green; **E–H**). Micrographs show that there is a loss of TH and DAT and a progressive loss of synapsin-driven Cre at 4 months. At 4 months, DAT staining appears fragmented and stains scattered fibers, whereas very few intact cell profiles (marked with arrowheads in **F** and **H**) can be identified in *cNurr1^{AAVCre}* mice (compare insets in **F**, **H**). Scale bar, 200 μ m.

progressive dysfunction characterized by a partial loss of the mDA neuron phenotype. Although we see few signs of neuronal degeneration, we cannot exclude a limited cell loss.

To assess whether the observed dysfunction was paralleled by an altered motor behavior, *cNurr1^{AAVCre}* mice were subjected to a stepping test at 3 and 4 months (Schallert et al., 1992; Kirik et al., 1998). Performance of the left forelimb (i.e., the limb contralateral to the vector injection) was impaired at both time points (Fig. 8). Additional behavioral testing, including amphetamine-induced rotations and a corridor test, indicated that individual mutant animals appeared affected; however, the *Nurr1*-ablated group did not show alterations that were statistically significant (supplemental Fig. 10, available at www.jneurosci.org as supplemental material). Our results demonstrate progressive mDA neuron dysfunction, leading to a more severe deficiency at 3–4 months after *Nurr1* ablation.

Discussion

This study provides definitive evidence that Nurr1 is not only critical for early differentiation but also for the maintenance of functional mDA neurons. Conditional gene targeting at late embryogenesis, when characteristic features of mDA neurons are already apparent, results in a rapid and close to complete mDA neuron loss. Only few TH-positive cells remain within the VTA also in the absence of Nurr1. Removal of Nurr1 leads to a severe dysfunction also in adult mDA neurons. It should be noted that reduction of striatal DA and the behavioral effects after adult ablation most likely underestimate the importance of Nurr1 in the adult brain because AAV injection only transduced a proportion of all mDA neurons in the injected side of treated animals. Thus, these data emphasize the importance of studying developmental mechanisms for elucidating neuron maintenance mechanisms. An analo-

gous example is provided by the glial cell line-derived neurotrophic factor (GDNF). GDNF is known to promote neuronal survival under development, but only recently has conditional gene targeting enabled studies that interrogate the role of GDNF and other factors signaling via Ret for maintenance of midbrain dopamine neurons in the adult brain (Oo et al., 2003; Jain et al., 2006; Kramer et al., 2007; Pascual et al., 2008).

Data presented here have implications for our understanding of how mature differentiated cell types are maintained. Previous studies have indicated that the differentiated state is not irreversible because even mature specialized cells, including for example, olfactory neurons and mature T- and B-cells, can be reprogrammed into undifferentiated pluripotent cells by either somatic cell nuclear transfer or using the recently developed methodology for the generation of induced pluripotent stem cells (Takahashi and Yamanaka, 2006; Gurdon and Melton, 2008). Nevertheless, under normal nonmanipulated conditions *in vivo*, differentiated cells are remarkably stable, indicating the importance of mechanisms that maintain cells in their appropriate differentiated state. Gene targeting in non-neural cell types has revealed how transcription factors functioning in development can be important for the maintenance of terminally differentiated cell types, e.g., Pax5 in B-lymphocytes and Prox1 in lymphatic endothelial cells (Cobaleda et al., 2007; Johnson et al., 2008). In CNS, transcription factors identified for their key roles in early neuron development often continue to be expressed in the adult brain and may therefore guard against loss of phenotype or drift into alternative states (Smidt et al., 1997, 2000; Zetterström et al., 1997; Hendricks et al., 1999; Vult von Steyrn et al., 1999; Albéri et al., 2004; Simon et al., 2004; Kang et al., 2007; Kittappa et al., 2007; Smidt and Burbach, 2007; Alavian et al.,

2008). However, remarkably little is known of how these factors function at late stages of development or in the adult. Although examples of adult mDA neuron loss has been reported in mice haploinsufficient for transcription factor genes such as *Engrailed* and *FoxA2*, it remains possible that defects originate during embryonic development (Albéri et al., 2004; Zhao et al., 2006; Kittappa et al., 2007; Sonnier et al., 2007). Importantly, *FoxA2* and *Engrailed* are critical for the establishment of the floor plate and for early midbrain/hindbrain development, respectively, and they are directly and indirectly affecting many cell fates along the entire neuraxis. Thus, haploinsufficiency may cause embryonic deficiencies that do not become manifest until adult stages, a possibility that emphasizes the importance of temporally controlled conditional gene targeting to rigorously test how transcription factors function in terminally differentiated neurons.

We do not yet understand why *Nurr1* is required in already differentiated mDA neurons. However, data presented here provide compelling evidence for the existence of “terminal selector genes” in mammalian CNS development. Such genes, defined from studies of *Caenorhabditis elegans* neuronal development, are continuously expressed throughout the life of neurons and are essential for both the establishment and maintenance of distinct neuronal phenotypes (Hobert, 2008). Thus, *Nurr1*, which probably regulates typical mDA neuron markers such as *TH*, *DAT*, *AADC*, and *VMAT2* (Sakurada et al., 1999; Sacchetti et al., 2001; Hermanson et al., 2003; Kim et al., 2003), is likely required for both early differentiation and maintenance by regulating genes that distinguish mDA neurons from other neuron types. Presumably, such regulation is critical throughout the life of mDA neurons and would depend on additional components, such as *Pitx3*, in a core transcription factor network (Jacobs et al., 2009).

How may dysregulated *Nurr1* activity contribute to PD? Studies in PD patients have shown that, in early stages of the disease, SNc cell bodies are relatively spared compared with the loss of DA in the putamen (Fearnley and Lees, 1991) and that a significant fraction of the surviving, pigmented, DA somata in the SNc have much reduced expression of the TH enzyme (Hirsch et al., 1988; Chu et al., 2006). This suggests that, during early stages of disease, nigral DA neurons may survive in a dysfunctional state characterized by a downregulated neurotransmitter machinery. An interesting possibility supported by our data is that reduced expression of *Nurr1* contributes to such symptoms. Indeed, *Nurr1* is severely reduced in neurons with signs of pathology in

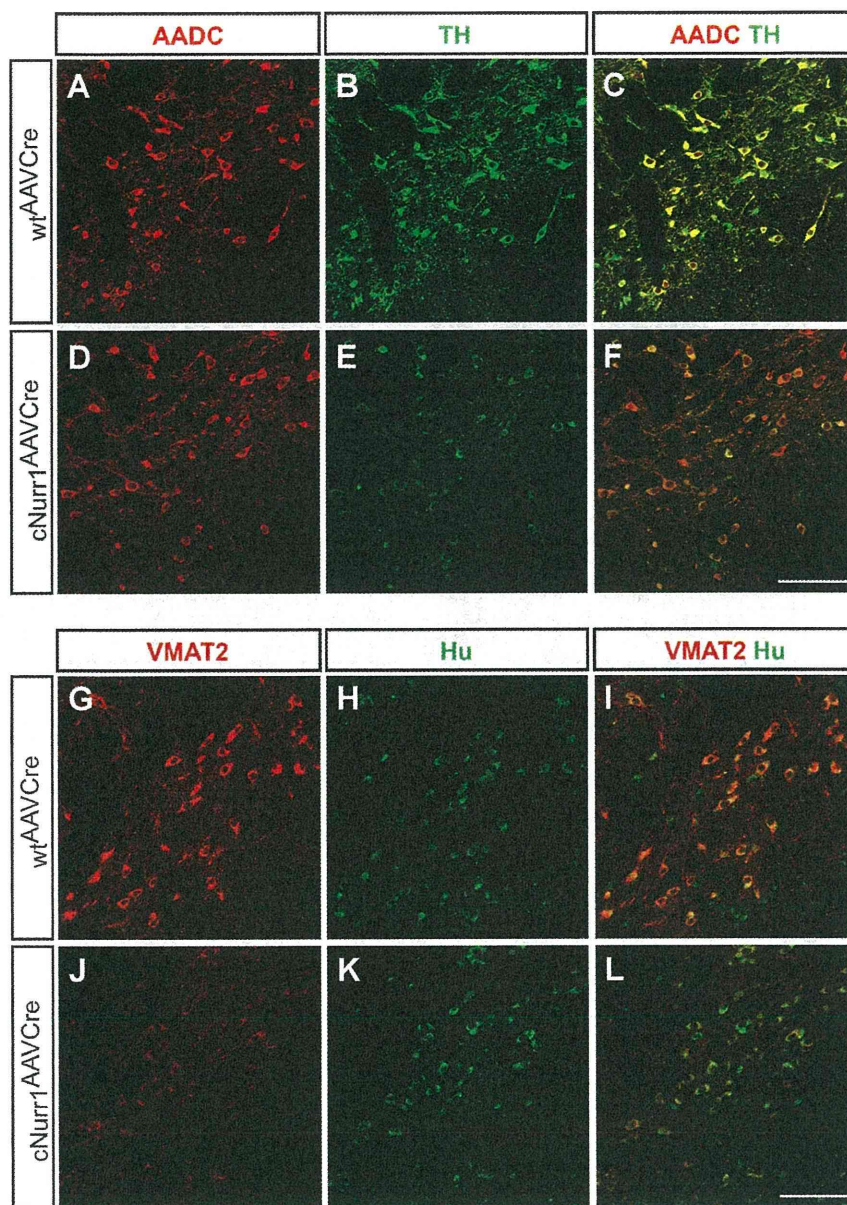


Figure 7. Decreased levels of VMAT2 but not AADC in *cNurr1^{AAVCre}* mice. Confocal analysis of SNc in *wtAAVCre* and *cNurr1^{AAVCre}* mice at 4 months, as indicated. **A–F**, Confocal images show staining of AADC (red; **A, D**), TH (green; **B, E**), and double staining of both markers (**C, F**). Micrographs show that AADC expression appears expressed at normal levels in most cells with decreased levels of TH. **G–L**, Confocal images show staining for VMAT2 (red; **G, J**), Hu (**H, K**), and double staining of both markers (**I, L**). Micrographs show that VMAT2 is severely decreased in *cNurr1^{AAVCre}* mice, whereas Hu is maintained at normal levels in essentially all cells with decreased VMAT2. Scale bar, 200 μ m.

PD brain tissue, and reduced *Nurr1* expression in patients' peripheral blood lymphocytes indicates that diminished *Nurr1* activity may be a systemic feature of disease (Chu et al., 2006; Le et al., 2008). Although such correlations do not determine whether reduced *Nurr1* expression is a cause or a consequence of disease, progressive cell dysfunction in *Nurr1*-ablated mice provides a clear indication that diminished *Nurr1* expression in PD should have deleterious consequences for patients. This view is supported by the identification of *Nurr1* gene variants that have been associated with rare cases of familial and sporadic PD (Xu et al., 2002; Le et al., 2003; Zheng et al., 2003; Jankovic et al., 2005; Grimes et al., 2006; Jacobsen et al., 2008). Although other studies have failed to identify such mutations and indicated that *Nurr1*

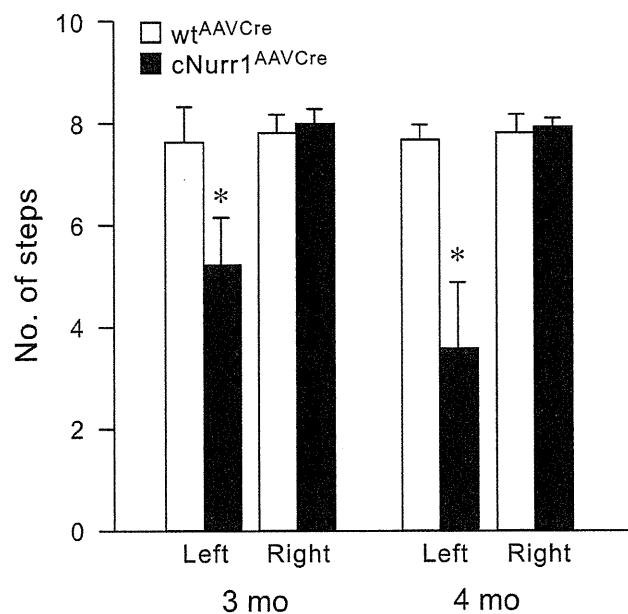


Figure 8. Forelimb akinesia in the stepping test. The performance of the left paw (contralateral to the vector injection) was significantly impaired in the fl/fl mice ($n = 16$) but not the wild-type mice ($n = 13$). Although the impairment was significant at both time points, 3 and 4 months after vector injection, their performance got significantly worse over time ($p < 0.01$, Student's paired t test): 15 of the 16 mice in the fl/fl group showed a decline in their stepping scores between the two tests, and at 4 months, 14 of the fl/fl mice had scores below 5 compared with 6 in the 3 month test. Scores give the means of steps recorded in the forehand and backhand direction for each paw (see Materials and Methods). * $p < 0.001$, Student's paired t test.

gene variants as a cause of PD must be very rare, the combined data from genetics, postmortem PD brain tissue analyses, and the ablation experiments reported here strongly imply that, if and when Nurr1 function is reduced, it will exaggerate PD progression and severity (Wellenbrock et al., 2003; Hering et al., 2004; Tan et al., 2004).

The results indicate that therapies that can restore Nurr1 activity in diseased but not yet degenerated mDA neurons could be of clinical relevance. We envision several strategies whereby Nurr1 activity could be increased. (1) Nurr1 belongs to the nuclear receptor family whose members are commonly regulated by small lipophilic ligands. The putative ligand binding domain of Nurr1 is unconventional and lacks a ligand-binding pocket, but Nurr1 forms heterodimers with retinoid X receptors (RXRs), and ligands activating these receptors can protect mDA neurons in culture (Wallen-Mackenzie et al., 2003; Wang et al., 2003). Thus, RXR may be a relevant target for ligand modulation of Nurr1-regulated processes. It will be important to investigate to what extent Nurr1–RXR heterodimers versus Nurr1 alone are important in pathways associated with the phenotype described in this paper. (2) Nurr1 activity is possible to modulate, for example, by the leukemia drug 6-mercaptopurine (Ordentlich et al., 2003). Although such drugs are pleiotropic and serious side effects are likely, other compounds with higher specificity may be possible to identify. (3) Therapies directed at increasing Nurr1 activity would be effective only as long as sufficient levels of Nurr1 are expressed in diseased neurons. Thus, treatments aimed at restoration of Nurr1 expression by gene delivery may prove advantageous. Using similar AAV vectors as administered in this study may be of particular interest because they have properties that are clinically favorable and are already used in clinical trials in PD patients (Check, 2007).

In conclusion, loss of Nurr1 at stages when characteristic features of mDA neurons are already apparent in the developing embryo or in fully differentiated adult neurons results in loss of mDA neuron-specific gene expression and neuron degeneration. These findings highlight the importance of developmental mechanisms also in the adult brain and clearly indicate that they may be critical for the understanding of cell maintenance and neurodegeneration. How Nurr1 and other transcription factors operate in adult neurons to control and prevent loss or drift in phenotype remains a challenge for future studies.

References

- Alavian KN, Scholz C, Simon HH (2008) Transcriptional regulation of mesencephalic dopaminergic neurons: the full circle of life and death. *Mov Disord* 23:319–328.
- Albéri L, Sgadò P, Simon HH (2004) Engrailed genes are cell-autonomously required to prevent apoptosis in mesencephalic dopaminergic neurons. *Development* 131:3229–3236.
- Andersson E, Tryggvason U, Deng Q, Friling S, Alekseenko Z, Robert B, Perlmann T, Ericson J (2006) Identification of intrinsic determinants of midbrain dopamine neurons. *Cell* 124:393–405.
- Breese GR, Knapp DJ, Criswell HE, Moy SS, Papadeas ST, Blake BL (2005) The neonate-6-hydroxydopamine-lesioned rat: a model for clinical neuroscience and neurobiological principles. *Brain Res Brain Res Rev* 48:57–73.
- Castillo SO, Baffi JS, Palkovits M, Goldstein DS, Kopin IJ, Witta J, Magnuson MA, Nikodem VM (1998) Dopamine biosynthesis is selectively abolished in substantia nigra ventral tegmental area but not in hypothalamic neurons in mice with targeted disruption of the Nurr1 gene. *Mol Cell Neurosci* 11:36–46.
- Check E (2007) Second chance. *Nat Med* 13:770–771.
- Chu Y, Le W, Kompolti K, Jankovic J, Mufson EJ, Kordower JH (2006) Nurr1 in Parkinson's disease and related disorders. *J Comp Neurol* 494:495–514.
- Cobaleda C, Jochum W, Busslinger M (2007) Conversion of mature B cells into T cells by dedifferentiation to uncommitted progenitors. *Nature* 449:473–477.
- Ekstrand MI, Terzioglu M, Galter D, Zhu S, Hofstetter C, Lindqvist E, Thams S, Bergstrand A, Hansson FS, Trifunovic A, Hoffer B, Cullheim S, Mohammed AH, Olson L, Larsson NG (2007) Progressive parkinsonism in mice with respiratory-chain-deficient dopamine neurons. *Proc Natl Acad Sci U S A* 104:1325–1330.
- Fearnley JM, Lees AJ (1991) Ageing and Parkinson's disease: substantia nigra regional selectivity. *Brain* 114:2283–2301.
- Grimes DA, Han F, Panisset M, Racacho L, Xiao F, Zou R, Westaff K, Bulman DE (2006) Translated mutation in the Nurr1 gene as a cause for Parkinson's disease. *Mov Disord* 21:906–909.
- Gurdon JB, Melton DA (2008) Nuclear reprogramming in cells. *Science* 322:1811–1815.
- Hendricks T, Francis N, Fyodorov D, Deneris ES (1999) The ETS domain factor Pet-1 is an early and precise marker of central serotonin neurons and interacts with a conserved element in serotonergic genes. *J Neurosci* 19:10348–10356.
- Hering R, Petrovic S, Mietz EM, Holzmann C, Berg D, Bauer P, Weitalla D, Müller T, Berger K, Krüger R, Riess O (2004) Extended mutation analysis and association studies of Nurr1 (NR4A2) in Parkinson disease. *Neurology* 62:1231–1232.
- Hermanson E, Joseph B, Castro D, Lindqvist E, Aarnisalo P, Wallén A, Benoit G, Hengerer B, Olson L, Perlmann T (2003) Nurr1 regulates dopamine synthesis and storage in MN9D dopamine cells. *Exp Cell Res* 288:324–334.
- Hirsch E, Graybiel AM, Agid YA (1988) Melanized dopaminergic neurons are differentially susceptible to degeneration in Parkinson's disease. *Nature* 334:345–348.
- Hobert O (2008) Regulatory logic of neuronal diversity: terminal selector genes and selector motifs. *Proc Natl Acad Sci U S A* 105:20067–20071.
- Huot P, Parent A (2007) Dopaminergic neurons intrinsic to the striatum. *J Neurochem* 101:1441–1447.
- Jacobs FM, van Erp S, van der Linden AJ, von Oerthel L, Burbach JP, Smidt MP (2009) Pitx3 potentiates Nurr1 in dopamine neuron terminal dif-

- ferentiation through release of SMRT-mediated repression. *Development* 136:531–540.
- Jacobsen KX, MacDonald H, Lemonde S, Daigle M, Grimes DA, Bulman DE, Albert PR (2008) A Nurr1 point mutant, implicated in Parkinson's disease, uncouples ERK1/2-dependent regulation of tyrosine hydroxylase transcription. *Neurobiol Dis* 29:117–122.
- Jain S, Golden JP, Wozniak D, Pehek E, Johnson EM Jr, Milbrandt J (2006) RET is dispensable for maintenance of midbrain dopaminergic neurons in adult mice. *J Neurosci* 26:11230–11238.
- Jankovic J, Chen S, Le WD (2005) The role of Nurr1 in the development of dopaminergic neurons and Parkinson's disease. *Prog Neurobiol* 77:128–138.
- Johnson NC, Dillard ME, Baluk P, McDonald DM, Harvey NL, Frase SL, Oliver G (2008) Lymphatic endothelial cell identity is reversible and its maintenance requires Prox1 activity. *Genes Dev* 22:3282–3291.
- Kang BJ, Chang DA, Mackay DD, West GH, Moreira TS, Takakura AC, Gwilt JM, Guyenet PG, Stornetta RL (2007) Central nervous system distribution of the transcription factor Phox2b in the adult rat. *J Comp Neurol* 503:627–641.
- Kim KS, Kim CH, Hwang DY, Seo H, Chung S, Hong SJ, Lim JK, Anderson T, Isacson O (2003) Orphan nuclear receptor Nurr1 directly transactivates the promoter activity of the tyrosine hydroxylase gene in a cell-specific manner. *J Neurochem* 85:622–634.
- Kirik D, Rosenblad C, Björklund A (1998) Characterization of behavioral and neurodegenerative changes following partial lesions of the nigrostriatal dopamine system induced by intrastriatal 6-hydroxydopamine in the rat. *Exp Neurol* 152:259–277.
- Kittappa R, Chang WW, Awatramani RB, McKay RD (2007) The *foxa2* gene controls the birth and spontaneous degeneration of dopamine neurons in old age. *PLoS Biol* 5:e325.
- Kramer ER, Aron L, Ramakers GM, Seitz S, Zhuang X, Beyer K, Smidt MP, Klein R (2007) Absence of Ret signaling in mice causes progressive and late degeneration of the nigrostriatal system. *PLoS Biol* 5:e39.
- Le W, Pan T, Huang M, Xu P, Xie W, Zhu W, Zhang X, Deng H, Jankovic J (2008) Decreased NURR1 gene expression in patients with Parkinson's disease. *J Neurol Sci* 273:29–33.
- Le WD, Xu P, Jankovic J, Jiang H, Appel SH, Smith RG, Vassilatis DK (2003) Mutations in NR4A2 associated with familial Parkinson disease. *Nat Genet* 33:85–89.
- Oo TF, Kholodilov N, Burke RE (2003) Regulation of natural cell death in dopaminergic neurons of the substantia nigra by striatal glial cell line-derived neurotrophic factor *in vivo*. *J Neurosci* 23:5141–5148.
- Ordentlich P, Yan Y, Zhou S, Heyman RA (2003) Identification of the anti-neoplastic agent 6-mercaptopurine as an activator of the orphan nuclear hormone receptor Nurr1. *J Biol Chem* 278:24791–24799.
- Pascual A, Hidalgo-Figueroa M, Piruat JJ, Pintado CO, Gómez-Díaz R, López-Barneo J (2008) Absolute requirement of GDNF for adult catecholaminergic neuron survival. *Nat Neurosci* 11:755–761.
- Perlmann T, Wallén-Mackenzie A (2004) Nurr1, an orphan nuclear receptor with essential functions in developing dopamine cells. *Cell Tissue Res* 318:45–52.
- Sacchetti P, Bronschid LA, Granneman JG, Bannon MJ (1999) Characterization of the 5'-flanking region of the human dopamine transporter gene. *Brain Res Mol Brain Res* 74:167–174.
- Sacchetti P, Mitchell TR, Granneman JG, Bannon MJ (2001) Nurr1 enhances transcription of the human dopamine transporter gene through a novel mechanism. *J Neurochem* 76:1565–1572.
- Sakurada K, Ohshima-Sakurada M, Palmer TD, Gage FH (1999) Nurr1, an orphan nuclear receptor, is a transcriptional activator of endogenous tyrosine hydroxylase in neural progenitor cells derived from the adult brain. *Development* 126:4017–4026.
- Saucedo-Cardenas O, Quintana-Hau JD, Le WD, Smidt MP, Cox JJ, De Mayo F, Burbach JP, Conneely OM (1998) Nurr1 is essential for the induction of the dopaminergic phenotype and the survival of ventral mesencephalic late dopaminergic precursor neurons. *Proc Natl Acad Sci U S A* 95:4013–4018.
- Schallert T, Norton D, Jones TA (1992) A clinically relevant unilateral rat model of Parkinsonian akinesia. *J Neural Transpl Plast* 3:332–333.
- Simon HH, Thuret S, Alberi L (2004) Midbrain dopaminergic neurons: control of their cell fate by the engrailed transcription factors. *Cell Tissue Res* 318:53–61.
- Smidt MP, Burbach JP (2007) How to make a mesodiencephalic dopaminergic neuron. *Nat Rev Neurosci* 8:21–32.
- Smidt MP, van Schaick HS, Lanctôt C, Tremblay JJ, Cox JJ, van der Kleij AA, Wolterink G, Drouin J, Burbach JP (1997) A homeodomain gene Ptx3 has highly restricted brain expression in mesencephalic dopaminergic neurons. *Proc Natl Acad Sci U S A* 94:13305–13310.
- Smidt MP, Asbreuk CH, Cox JJ, Chen H, Johnson RL, Burbach JP (2000) A second independent pathway for development of mesencephalic dopaminergic neurons requires Lmx1b. *Nat Neurosci* 3:337–341.
- Smidt MP, Smits SM, Burbach JP (2004) Homeobox gene Pitx3 and its role in the development of dopamine neurons of the substantia nigra. *Cell Tissue Res* 318:35–43.
- Snyder AM, Zigmond MJ, Lund RD (1986) Sprouting of serotonergic afferents into striatum after dopamine-depleting lesions in infant rats: a retrograde transport and immunocytochemical study. *J Comp Neurol* 245:274–281.
- Sonnier L, Le Pen G, Hartmann A, Bizot JC, Trovero F, Krebs MO, Prochiantz A (2007) Progressive loss of dopaminergic neurons in the ventral mid-brain of adult mice heterozygote for Engrailed 1. *J Neurosci* 27:1063–1071.
- Soriano P (1999) Generalized lacZ expression with the ROSA26 Cre reporter strain. *Nat Genet* 21:70–71.
- Takahashi K, Yamanaka S (2006) Induction of pluripotent stem cells from mouse embryonic and adult fibroblast cultures by defined factors. *Cell* 126:663–676.
- Tan EK, Chung H, Chandran VR, Tan C, Shen H, Yew K, Pavanni R, Puvan KA, Wong MC, Teoh ML, Yih Y, Zhao Y (2004) Nurr1 mutational screen in Parkinson's disease. *Mov Disord* 19:1503–1505.
- Vult von Steyern F, Martinov V, Rabben I, Njå A, de Lapeyrière O, Lomo T (1999) The homeodomain transcription factors Islet 1 and HB9 are expressed in adult alpha and gamma motoneurons identified by selective retrograde tracing. *Eur J Neurosci* 11:2093–2102.
- Wallen-Mackenzie A, Mata de Urquiza A, Petersson S, Rodriguez FJ, Friling S, Wagner J, Ordentlich P, Lengqvist J, Heyman RA, Arenas E, Perlmann T (2003) Nurr1-RXR heterodimers mediate RXR ligand-induced signaling in neuronal cells. *Genes Dev* 17:3036–3047.
- Wang Z, Benoit G, Liu J, Prasad S, Aarnisalo P, Liu X, Xu H, Walker NP, Perlmann T (2003) Structure and function of Nurr1 identifies a class of ligand-independent nuclear receptors. *Nature* 423:555–560.
- Wellenbrock C, Hedrich K, Schafer N, Kasten M, Jacobs H, Schwinger E, Hagenah J, Pramstaller PP, Vieregge P, Klein C (2003) NR4A2 mutations are rare among European patients with familial Parkinson's disease. *Ann Neurol* 54:415.
- Xu PY, Liang R, Jankovic J, Hunter C, Zeng YX, Ashizawa T, Lai D, Le WD (2002) Association of homozygous 7048G7049 variant in the intron six of Nurr1 gene with Parkinson's disease. *Neurology* 58:881–884.
- Zetterström RH, Williams R, Perlmann T, Olson L (1996) Cellular expression of the immediate early transcription factors Nurr1 and NGFI-B suggests a gene regulatory role in several brain regions including the nigrostriatal dopamine system. *Brain Res Mol Brain Res* 41:111–120.
- Zetterström RH, Solomin L, Jansson L, Hoffer BJ, Olson L, Perlmann T (1997) Dopamine neuron agenesis in Nurr1-deficient mice. *Science* 276:248–250.
- Zhao ZQ, Scott M, Chiechio S, Wang JS, Renner KJ, Gereau RW 4th, Johnson RL, Deneris ES, Chen ZF (2006) Lmx1b is required for maintenance of central serotonergic neurons and mice lacking central serotonergic system exhibit normal locomotor activity. *J Neurosci* 26:12781–12788.
- Zheng K, Heydari B, Simon DK (2003) A common NURR1 polymorphism associated with Parkinson disease and diffuse Lewy body disease. *Arch Neurol* 60:722–725.

The current status of gene therapy for Parkinson's disease

Shin-ichi Muramatsu, M.D, Ph.D

Division of Neurology, Department of Medicine, Jichi Medical University, 3311-1 Yakushiji, Shimotsuke, Tochigi 329-0498, JAPAN

ABSTRACT

The recent development of viral vectors, especially vectors derived from adeno-associated virus (AAV), has translated gene therapy for Parkinson's disease (PD) from animal experiments into clinical trials. The current gene therapy protocols used are based on three major strategies. The first protocol involves local production of dopamine via the introduction of dopamine-synthesizing enzyme genes into the putamen. The aromatic L-amino acid decarboxylase (AADC) gene has been transferred in this manner with the aim of efficiently converting orally administered L-dopa. The delivery of triple genes including tyrosine hydroxylase (TH), guanosine triphosphate cyclohydrolase I (GCH) and AADC is also being undertaken, and is aimed at continuously supplying dopamine into the putamen. The second protocol involves the protection of nigrostriatal projections via the production of neurturin, a trophic factor for dopaminergic neurons in the putamen. The final method includes the modulation of neural activity along the output pathway of the basal ganglia by transducing the subthalamic nucleus with vectors expressing glutamic acid decarboxylase (GAD-65, GAD-67), a key enzyme required for the synthesis of the inhibitory transmitter γ -aminobutyric acid (GABA). The initial results of phase 1 studies using AAV vectors have not only confirmed the safety of these vectors, but have also revealed the alleviation of motor symptoms associated with PD.

KEY WORDS: Adeno-associated virus, Aromatic L-amino acid decarboxylase, Neurturin, Glutamic acid decarboxylase, Positron emission tomography
Corresponding Author: Shin-ichi Muramatsu, M.D, Ph.D, E-mail: muramats@jichi.ac.jp; Tel: + 81-285-58-7352, Fax: + 81-285-44-5118

doi : 10.5214/ans.0972-7531.1017209

Introduction

Almost two decades have passed since the first gene therapy clinical trial was conducted for the treatment of adenosine deaminase deficiency at the National Institute of Health in the United States in 1990. Although gene therapy appeared to be a ground breaking form of medical treatment at the time, it has not proven to be as successful in treating disease as initially anticipated. A patient with ornithine transcarbamylase deficiency died of systemic inflammatory response syndrome

(SIRS) following the administration of a large quantity of adenoviral vector into the hepatic artery.¹ In addition, some children with X-linked severe combined immunodeficiency (X-SCID) developed leukemia due to the activation of an oncogene after gene therapy using a retroviral vector.^{2,3} These reports describing the severe, adverse effects of gene therapy dampened the excitement underlying the success of gene therapy treatment to some extent. However, encouraging results have been obtained more recently with clinical studies for Parkinson's disease (PD).⁴⁻⁷

Table. Gene therapy clinical trials for Parkinson's disease.

Gene	AADC		TH/GCH/AADC	Neurturin		GAD	
Function	Convert L-dopa to dopamine		Synthesis of dopamine from tyrosine	Neurotrophic factor for dopaminergic neurons		Synthesis of inhibitory neurotransmitter GABA	
Vector	AAV		EIAV	AAV		AAV	
Phase	I		I	I	II	I	II
Institute	UCSF ⁷	JMU	Henri Mondor Hospital ²²	UCF ⁵	Multi-center ²⁶	NYP Hospital ⁵	Multi-center
Dose	9x10 ¹⁰ 3x10 ¹¹	3x10 ¹¹	1x 2x	1.3x10 ¹¹ 5.4x10 ¹¹	5.4x10 ¹¹ Sham	3.5x10 ⁸ 1x10 ⁹ 3.5x10 ¹⁰	1x10 ¹¹ Sham
Number of subjects	10	6	6	12	54	12	40
Target	Putamen (Bilateral)		Putamen (Bilateral)	Putamen (Bilateral)		STN (Unilateral)	STN (Bilateral)
PET tracer	[¹⁸ F] fluoro-m-tyrosine			[¹⁸ F] fluoro-DOPA		[¹⁸ F] fluoro-deoxyglucose	

AADC, aromatic L-amino acid decarboxylase; AAV, adeno-associated virus; EIAV, equine infectious anemia virus; GABA, γ -aminobutyric acid; GAD, glutamic acid decarboxylase; GCH, guanosine triphosphate cyclohydrolase I; TH, tyrosine hydroxylase; STN, subthalamic nucleus. Dose of AAV vectors are represented as vector genome/patient.